University of Stavanger

FACULTY OF SCIENCE AND TECHNOLOGY

MASTER'S THESIS

Study programme/specialization: MSc. Petroleum Engineering: Process and Production Engineering	Spring semester, 2022 Open
Author: Muhammed Ahmed Salar Wali	.... Muhammed Ahmed Salar Wali

Programme coordinator: Øystein Arild Supervisors: UiS - Prof. Rune Wiggo Time

Title of master's thesis: EXPERIMENTAL ANALYSIS OF MULTI-PHASE FLOWS IN ORIFICE

Credits: 30

Keywords: Orifice metering, Multi-phase flow, Flow Mechanisms, Turbulent Models, Accumulation, Pressure Drop.	Number of pages: 58 + supplemental material/other: 7 Stavanger, 15th June 2022

Muhammed Ahmed Salar Wali

EXPERIMENTAL ANALYSIS OF MULTI-PHASE FLOWS IN ORIFICE

Universitetet
i Stavanger

In order to understand the behavior of multi-phase flow through orifices in horizontal pipes, an experimental approach is applied that utilizes the available flow rig in the multi-phase flow laboratory at the University of Stavanger. A test pipe of 0.7m was created that would allow easy changing of orifices. Several different geometries were used in the pipe to compare flow mechanisms at different flow rates. Superficial velocities for water ranged from 0.35 to 0.75 m/s and from 0.04 m/s to 0.1 m/s for air. Pressure drop across orifice was measured, and a video system was used in order to obtain images of flow under selected conditions.

Orifice meters have been widely used in single-phase metering. However, a simplistic approach to understand multi-phase flow has been applied. Therefore, in addition to understanding fluid dynamics in single-hole orifice a multi-hole orifice is also used. It is observed that to some extent pressure fluctuations are reduced when using a multi-hole orifice plate. Therefore, a hypothesis involving multiple jets that reduce the overall disturbance is made.

The recorded pressure drop signals give insights into the flow behavior, and results indicated that at higher pressure drops, a significant amount of air flows through orifice. Hence, the results of this study have demonstrated an ability to visualize flow disturbances across orifice plates with cheaper materials and replicate the industrial process in the multi-phase flow lab.

Acknowledgments

List of Abbreviations

CFD	Computational Fluid Dynamics
DAS	Data Acquisition System
EDR	Equivalent diameter ratio
ISO	International Organization for Standardization
NFOGM	Norwegian Society for Oil and Gas Measurement
MOV	Multiple Orifice Valve
MFM	Multi-phase Flow metering
PPE	Personnel Protective Equipment
SLPM	Standard liters per minute

Nomenclature

$P1$	Upstream Pressure
$P2$	Downstream Pressure
ΔP	Pressure Drop
U_p	Flow Velocity
U_{Ls}	Superficial Velocity of Liquid
U_{Gs}	Superficial Velocity of Gas
q_L	Liquid FLow Rate
q_G	Gas Flow rate
U_{mix}	Mixture Velocity
λ_L	No slip Fraction Liquid
λ_G	No slip Fraction Gas
S	Slip
ε_L	True Fraction liquid
D_p	Pipe Diameter
D_h	Orifice diameter
t	Thickness
T	Time
ρ	Density
ρ_m	Mixture Density
μ	Viscosity
Re_p	Reynolds Number
Re_m	Mixture Reynolds Number
M	Mach Number
γ	Liquid Holdup
β	Porosity
C_d	Discharge Coefficient
Q_t	Two phase Flow rate
X	LockHart Martinelli Two phase multiplier
x	Gas Quality

Table of Contents

List of Figures

List of Tables

Chapter 1

Introduction

1.1 Background

Flow measurement has been a critical process in many industries. It is vital to conduct investigations and detailed analyses of flow occurring in any pipe at any given time. The method of monitoring flow rate dates back to the stone age. However, a milestone in the theory of fluid flow and behavior came from Daniel Bernoulli in his famous work "Hydrodynamica" [Bernoulli, 1738]. Since then, the fluid flow has been a point of interest for many researchers, and numerous experimental and numerical analyses have been made to characterize and evaluate flow. In industries such as petroleum, power generation, pharmaceutical, nuclear, and food processing, there is a flow of material. Measuring flow is essential in a process or system; it could include pressurized water reactors [Orea et al., 2020], deep water oil spills [Osman and Ovinis, 2020], wastewater treatments [Kiss and Patziger, 2018], pump systems [Melzer et al., 2020], and many more. The measurement depends upon several parameters that include material and its conditions, type of flow, pressure, volume, temperature, and many more, as shown in Figure 1.1.

In most applications, the type of flow is essential. It could range from laminar to turbulent depending on flow rates and velocities; several flow types will be discussed in Chapter 2 as part of the literature review. Determining fluid rates and conditions is paramount to ensuring a system's safe, smooth, and cost-effective operation.

This study investigates the effect of single phase and two-phase flow through an orifice (single
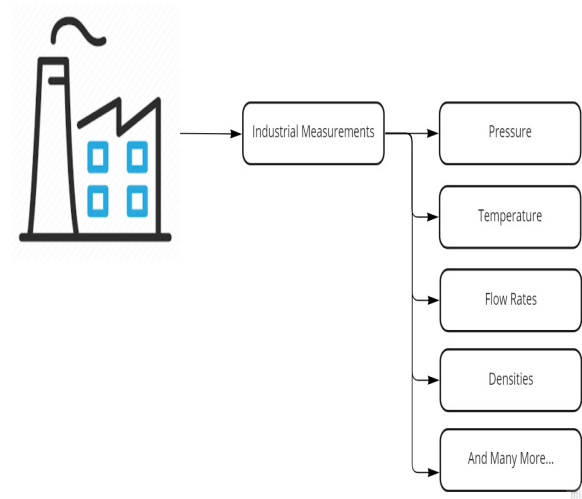
Figure 1.1: Variables measured in industries.

hole and multi hole) inside a pipe. An orifice is a device conventionally used to measure flow rates in fluid channels [Miller, 2014]. An orifice plate works on the principle of creating a sudden change in the cross-sectional area of the pipe channel. Following the law of conservation of mass, the fluid present inside needs to accelerate to pass through the changed geometry. The rise in flow velocity is followed by a drop in static pressure as per the conservation of energy. Widely, the drop in static pressure is used to measure the flow rate when using orifice plates. The permanent pressure loss that occurs after fluid passes through the orifice is associated with the geometric properties of an orifice. The pressure losses as shown in 1.2 are extensively discussed in several fluid dynamics books and the reader is referred to Frank M. White Fluid Dynamics [White, 2011].
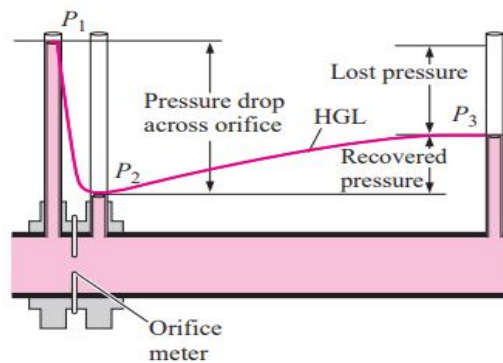
Figure 1.2: Pressure drop across orifice.[ÇENGEL, 2007]

Fluid flow in most pipelines is found to be turbulent. A natural property of turbulent flow is

that it creates disturbances and unsteadiness. These disturbances are further increased when there is more than one fluid flowing (multi-phase). Two-phase or multi-phase flow has been investigated extensively to clearly understand the nature of it, and at best, meter it. This leads us to the motivation behind this experimental study.

1.2 Motivation

Orifice meter has been one of the widely used flow metering devices in many process industries. However, most applications have been limited to single-phase flow for an orifice. The objective of the current investigation is to aid in understanding of multi-phase flow through orifice (air and water) that induce a pressure drop. Furthermore, research into multi-phase flow mechanism is necessary to visualize the phenomenons that are occurring inside a pipe that contains a restriction (such as an orifice)

It is essential to analyze several parameters involved and understand the nature of flow occurring. The work done at the University of Stavanger in the Multi-phase flow Laboratory can eventually be used to develop an optimum system to measure multi-phase flow. This thesis aims to describe results from experimental evaluations that help us to understand the objective mentioned above.

1.3 Outline of the thesis

This document is divided into six Chapters. Figure 1.3 presents an overview of chapters that form the sections of this thesis.

- Chapter 2 includes the necessary knowledge to understand multi-phase flow and orifice meters. Including some explanations and terminologies used are described in section 2.2.1.

- Chapter 3 discusses the approach taken to research and the motivation for the experiments conducted.

- A concise description of the experimental setup and instrumentation is also discussed in Chapter 4, including the investigations and challenges.

- The hypothesis and results, including the characteristics of flow and pressure measurements obtained, are discussed in Chapter 5.

- Chapter 6 lays out closing remarks and the conclusion for this document. Finally, a brief review of results and scope for further studies is explored.
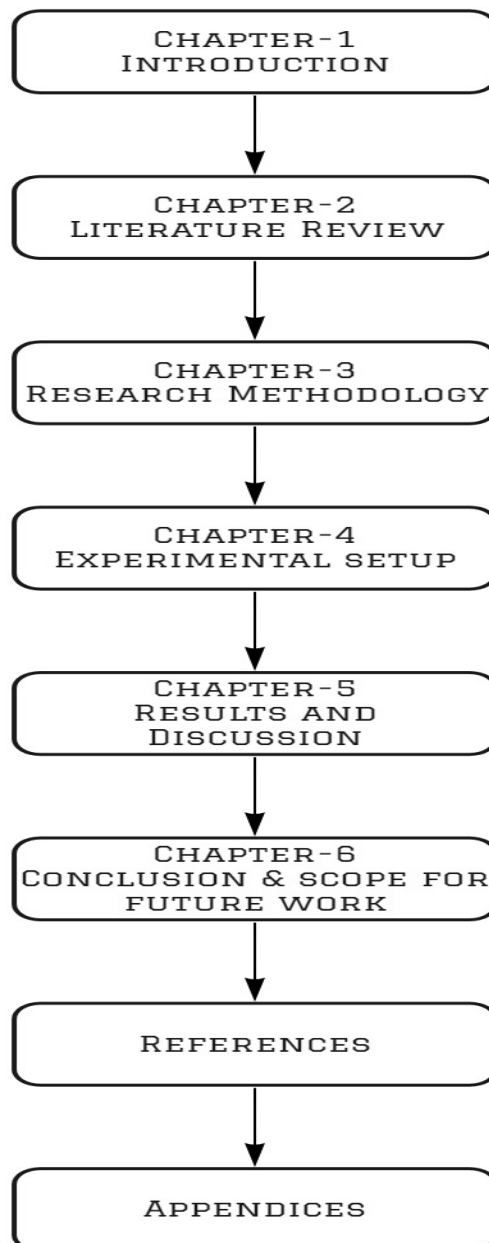
Figure 1.3: Outline of the thesis.

Chapter 2

Literature Review

This chapter summarizes the relevant research on multi-phase flow, specifically two-phase flow through an orifice. A significant portion of this chapter discusses terms and definitions used in multi-phase flow metering distinctively for orifice meters.

The nomenclature/abbreviations used by authors have been represented as the same in their research. Thus, variables could differ from those described in this chapter.

2.1   Introduction to Multi-phase flow

Before continuing on the investigation of multi-phase flow metering (MFM) using orifice, it is essential to understand the basics of multi-phase flow.

Multi-phase flow analysis has been a focus for several scientists in different disciplines: mechanical, nuclear, petroleum, civil and chemical. As stated by Christopher E. Brennen in his book "Fundamentals of Multi-phase flow" [Brennen, 2005]

> *Virtually every processing technology must deal with multiphase flow, from cavitating pumps and turbines to electrophotographic processes to papermaking to the pellet form of almost all raw plastics*

In short, multiphase flows are the most common flows occurring in nature as well. From blood flow in our veins to flow that occurs when a person coughs. The simplest case of multiphase flow is a two-phase flow consisting of the same pure component in two different phases, such as

steam-water flow. Similarly, other chemical substances, such as air-water flow, are also known as two-phase flow. This air-water flow is the primary focus in this investigation.

2.1.1   Types of Multiphase flows, flow patterns and flow regimes maps

Building on the previous section 2.1, the main types of flow encountered in process industry depend on the following factors:

- Operating conditions (pressure and temperature).

- Physical properties of the conduit i.e. pipe diameter, shape, roughness, inclination.

- Phase properties i.e. velocities,viscosity and density.

- Several kinds of pipe work (bends,valves etc).

- Type of material flowing (solid, liquid or gaseous).

- Type of flow i.e. steady, pseudo steady or transient.

For a single-phase, the flow is discriminated by being laminar or turbulent. However, for two-phase flow, we differentiate between flow patterns and flow regimes that are distinctive in gas and liquid flow for a given time and space.

Visual observations were used to classify the flow patterns in two-phase flow experiments in laboratories, and the so-called "Flow pattern maps" such as Figures 2.1 and 2.2 were developed.

In the 1980s, intensive flow modeling efforts were made. The investigations of flow patterns for different pipe inclinations and diameters, operating pressure and rates, and the boundaries between regimes were determined. Several investigators used different variables for their maps, the most common being superficial velocities and mass flow rates that include horizontal pipe investigations from J.M. Mandhane [Mandhane et al., 1974] for gas-liquid. Dukler and Taitel [Dukler and Taitel, 1986] investigated the transitions in similar systems, and a further model for the prediction of flow-pattern transition was given by Barnea [Barnea, 1987]. As advancements in computing grew, so did the use of computational fluid dynamics (CFD). Many research

projects utilized CFD to solve practical fluid problems. Hence, several commercial software came to the market to solve multiphase modeling and simulations.

2.1.2   Gas-Liquid Flows

Flow regimes in a gas-liquid flow are complex. Several factors that govern flow regimes include; density of gas and liquid, viscosity, surface tension, wetting, dispersion, coalescence, body forces, and heat flux effects [Falcone, 2009]. Figures 2.3 and 2.4 illustrate flow regime transitions dependent on superficial gas and liquid velocities in horizontal and vertical flow. The regimes in horizontal pipes (Figure 2.1) are as follows:

- **Bubble flow**

  In such a flow, the bubbles are dispersed in the liquid phase. Due to the buoyancy effect, the bubbles tend to settle in the upper part of the pipe, as shown in figure 2.1.

- **Stratified flow**

  Gravitational separations occur at particular flow rates. The liquid starts to flow along the bottom of the pipe, and gas in the top part

- **Wavy flow**

  When gas velocity increases, waves are formed at the gas-liquid interface creating a wavy flow regime.

- **Plug flow**

  Bullet-shaped bubbles tend to flow along the top part of the pipe due to the buoyancy effect. It is also known as elongated bubble flow.

- **Slug flow**

  A passage along the channel fills the cross-section of the pipe, creating 'slugs.' These slugs can often be enormous and cause more significant disturbances in the flow.

- **Annular flow**

Here the liquid flows near the top and bottom of the wall at very high gas velocities. As a result, some liquid droplets are floating in the gas zone, as seen in figure 2.1. It can also be associated with wet-gas flows.
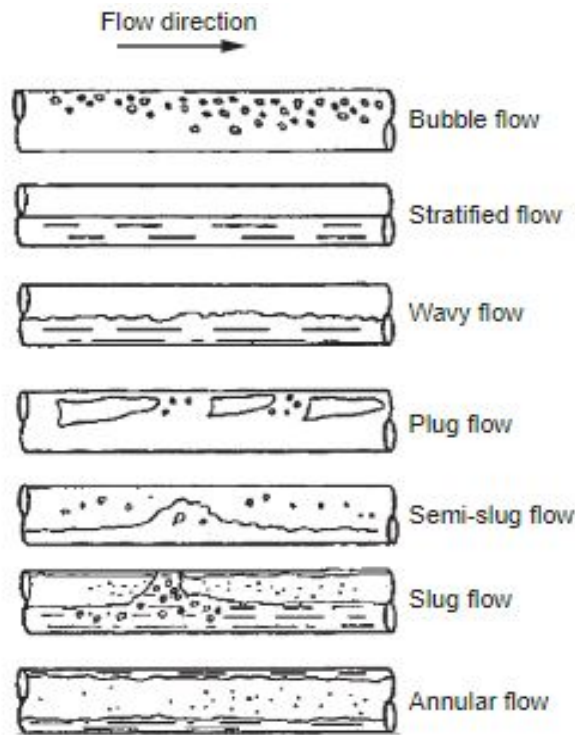
Figure 2.1: Flow patterns in horizontal flow [Falcone, 2009]

The gas-liquid flows regimes in vertical pipes illustrated in figure 2.2 are as follows

- **Bubble flow**

  The liquid is continuous, and dispersed bubbles flow within the liquid. The sizes of bubbles are generally non-uniform.

- **Slug/Plug flow**

  Such flow occurs when bubbles become large enough to take the channel/pipe size. Then, a bullet shape is observed with a combination of smaller dispersed bubbles.

- **Churn flow**

  At higher velocities, slugs tend to break down, leading to unstable flow regimes and an oscillatory motion of flow occurs.

- **Annular flow**

  Like horizontal flow, the liquid is attached to the walls, with gas moving at higher velocities.
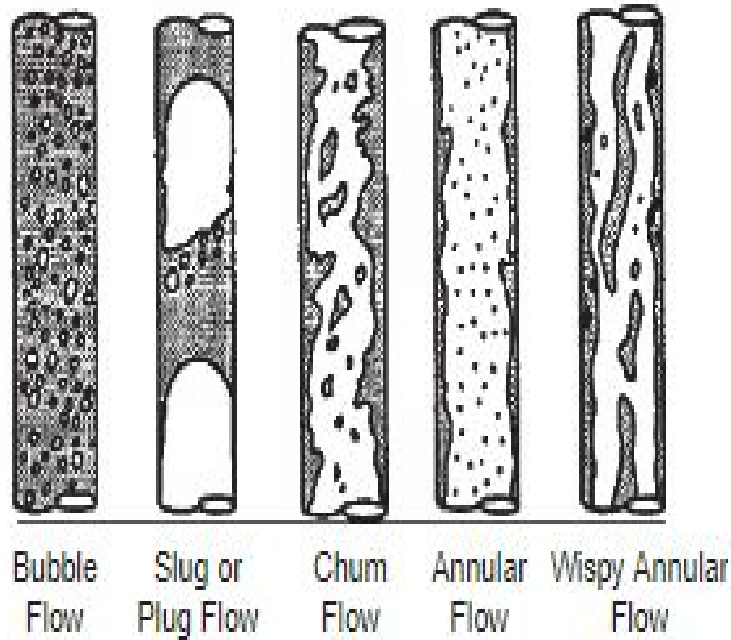
Figure 2.2: Flow patterns in Vertical flow [Falcone, 2009]

2.1.3   Flow regime maps

At first, J.M. Mandane [Mandhane et al., 1974] and later Taitel and Dukler [Dukler and Taitel, 1986] developed a flow regime map for both horizontal and vertical describing transitions in gas-liquid systems, as shown in figures 2.3 and 2.4.As from the flow regime maps a term superficial velocity is used.

Superficial velocities

Superficial velocity is a term often used in the axes of flow regime maps. They are defined as:

$$U_{LS} = \frac{q_L}{A}, U_{GS} = \frac{q_G}{A} \tag{2.1}$$

Where U_{Ls} and U_{Gs} are superficial/apparent velocities. The physical interpretation is simply the volumetric flow rate over the pipe's cross-sectional area. Hence the sum of superficial velocities

is known as mixture velocity, which is represented below.

$$U_{mix} = U_{LS} + U_{GS} \tag{2.2}$$

However, this is a derived velocity and only has a meaningful value if the flow is homogeneous and no-slip.
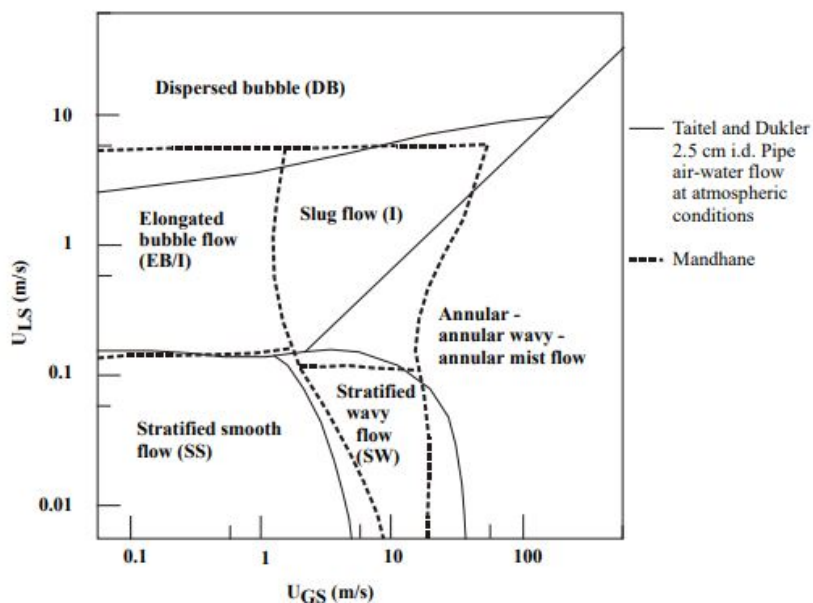
Figure 2.3: Horizontal pipe flow regime map [Dukler and Taitel, 1986]
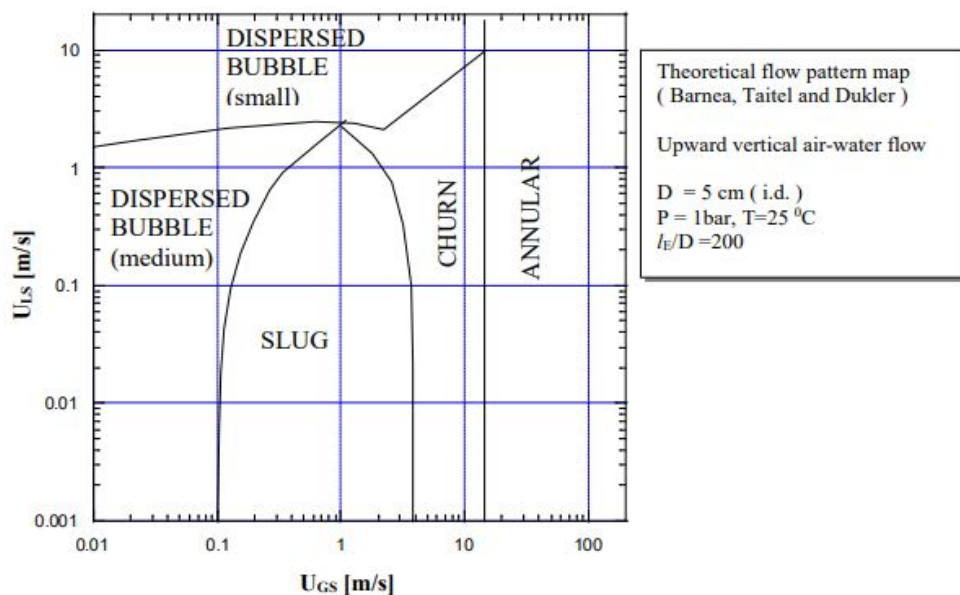
Figure 2.4: Vertical pipe flow regime map [Barnea, 1987]

No-slip and Slip

Often we are unsure of the dynamics of the flow. Hence, it is impossible to measure the fraction of phases present in any particular instance, e.g., in a subsea pipeline. However, it is crucial to predict the fluid fractions provided we know the volumetric flow rates q_L or q_G . We can calculate the no-slip fraction as

$$\lambda_L = \frac{q_L}{q_L + q_G},$$
(2.3)

$$\lambda_G = \frac{q_G}{q_L + q_G}$$
(2.4)

On the other hand, if slip is present, the phase velocities (U_{Ls} and U_{Gs}) would be different. The fluid fraction is different from the no-slip fraction as it is necessary to determine the actual flowing cross-sections A_L or A_G for liquid and gas. True liquid fraction is:

$$\varepsilon_L = \frac{A_L}{A} = \frac{A_L}{A_L + A_G}$$
(2.5)

Considering phase velocities:

$$U_{LS} = \frac{q_L}{A_L}$$

$$U_{GS} = \frac{q_G}{A_G}$$

Knowing

$$S = \frac{U_G}{U_L}$$
(2.6)

Indicating that

$$\varepsilon_L = \frac{q_L}{q_L + \frac{1}{S} \cdot q_G} = \frac{U_{LS}}{U_{LS} + \frac{1}{S} \cdot U_{GS}}$$

where S is the slip ratio, and we get

$$\varepsilon_G = \frac{q_G}{S \cdot q_L + q_G} = \frac{U_{GS}}{S \cdot U_{LS} + U_{GS}}$$
(2.7)

And when S $= 1$, the no slip fractions are equal to true slip fraction $\varepsilon_G = \lambda_G$ and $\varepsilon_L = \lambda_L$.

More representative flow regime maps are shown in figures 2.5 and 2.6
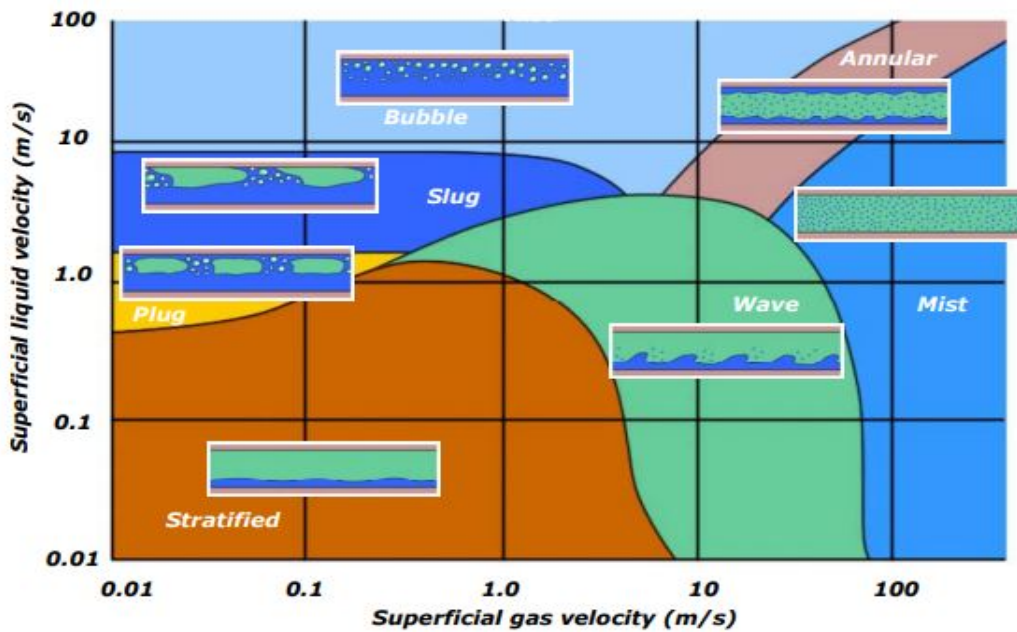
Figure 2.5: A generic two-phase horizontal flow map [NFOGM, 2005]
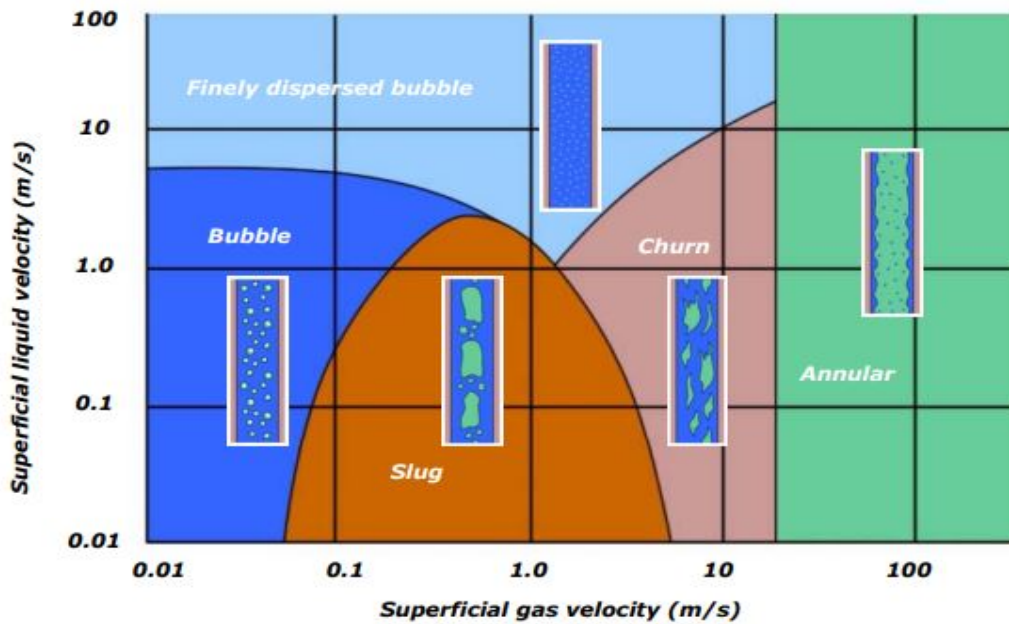
Figure 2.6: A generic two-phase vertical flow map[NFOGM, 2005]

2.1.4   The Coanda Effect

The so called Coanda effect is a fluid dynamics phenomenon that occurs whenever a jet flows from a nozzle. An example is shown in Figure 2.7, the jet from the nozzle is drawn to the closest wall. This mainly due to the back flow near-by wall[Time, 2017]. A drop in pressure

between jet and the wall forces the jet to move towards the wall. If multiple jets are flowing the pressure between the two jets is lowered due to the re-circulation zone and the jets merge into one another and flow as a single jet.
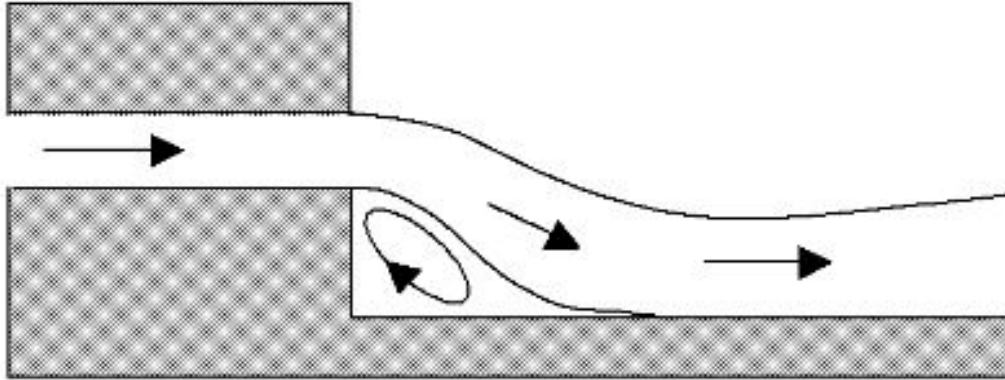
Figure 2.7: The Coanda Effect [Time, 2017]

2.2 Orifice Metering

Orifice meters are widely used for single-phase flow measurement [Falcone, 2009]. However, prior to indulging in orifice metering of two phases, we must establish some understanding of terminologies frequently used in this literature.

2.2.1 Terminologies

Considering a pipe of diameter $D_p(m)$ through which an in-compressible fluid of density $\rho(kg/m^3)$ and dynamic viscosity $\mu(Pa.sec)$, flowing at velocity $U_p(m/sec)$. An orifice (restriction) having hole dia. D_h and outer diameter is the same as the pipe's inner diameter. The geometric variables of the single and multi-hole orifice are shown in Figures 2.8 and 2.9. The orifice has a thickness t, and has N_h (number of holes) of diameter D_h.

A wide variety of terminology is found in the literature, and some practical terms are defined below to aid some understanding of this document.
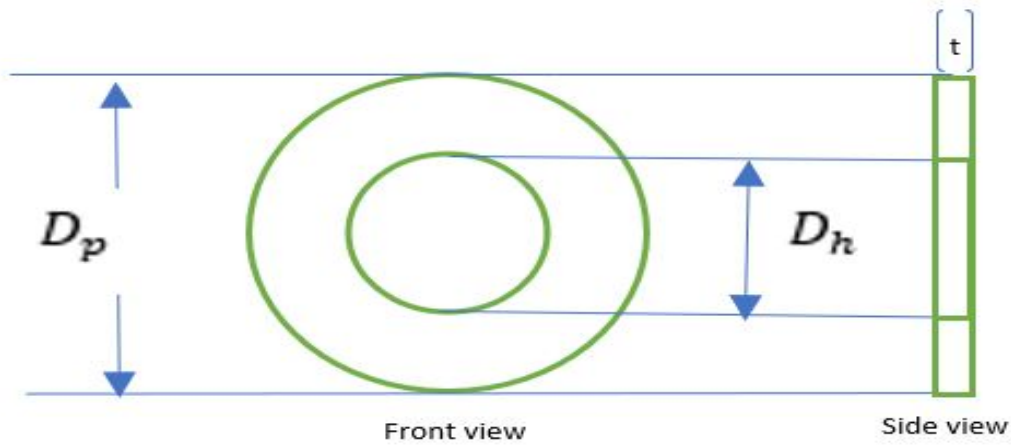
Figure 2.8: Single-Hole Orifice
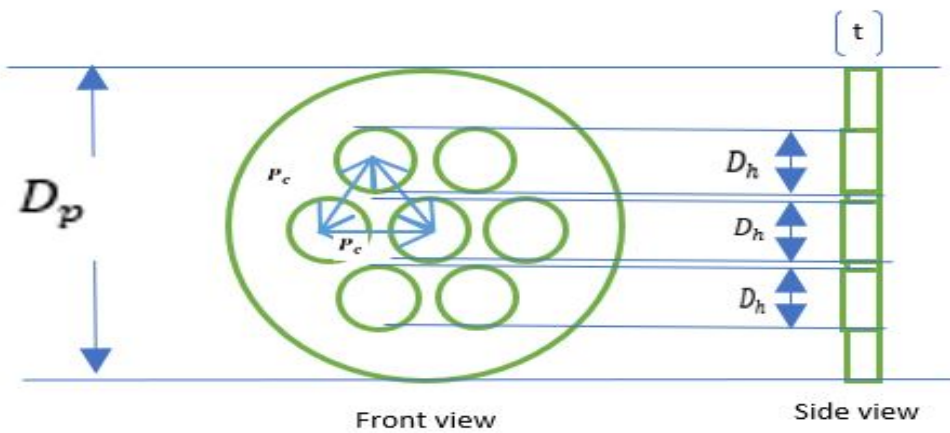
Figure 2.9: Multi-hole Orifice

Reynolds Number Re_h

It can be described as a dimensionless quantity representing the ratio of fluid momentum and the inertia force (shear). Fluid density and viscosity are a function of the Reynolds number. A higher Reynolds number suggests [Guo and Ghalambor, 2005] a free-flowing stream, and a lower number suggests a highly viscous or resisting stream.

Reynolds number for single-phase system can be defined as:

$$Re_p = \left(\frac{\rho U_p D_p}{\mu} \right) \tag{2.8}$$

Flow meters are essentially designed to operate in a turbulent flow. Around 95 percent of the time, flow is turbulent in closed conditions [Altendorf, 2006]. Flow is laminar when Re is below 2000. Above 4000, the flow is turbulent. Between these two values, the flow is generally

in transition.

Multiphase Reynolds number

As mentioned earlier, the calculation of the Reynolds number identifies the flow patterns that affect all measurements. In the case of two-phase flows, a multiphase Reynolds number should be defined from which a multiphase pattern can also be identified. In addition, the multiphase Reynolds number would enable the classification of the Discharge coefficient (Eq. 2.12) under multiphase conditions. For a no-slip, homogeneous flow with mixture velocity U_m, density ρ_m and viscosity μ_m, following mixing rules and known phase fractions and phase properties, the mixture Reynolds number can be defined as;

$$Re_m = \left(\frac{\rho_m U_m D_p}{\mu_m} \right) \tag{2.9}$$

Hagedorn and Brown [Hagedorn and Brown, 1965] proposed the following expression for mixture Reynolds number using empirical correlation for oil and gas wells as:

$$\mathrm{Re_m} = \frac{\rho_\mathrm{m} U_\mathrm{m} D}{\mu_l^\gamma \mu_\mathrm{g}^{(1-\gamma)}} \tag{2.10}$$

Where μ_l and μ_g are liquid and gas viscosities. γ, the liquid holdup, is defined as the ratio of liquid volume to the total volume of the pipe. Accurate measurements of the Reynolds number are necessary to calculate the frictional pressure drop that occurs in a flow. Hence, tailored models of mixture Reynolds number are required to model the phenomenons involved accurately.

Porosity (β)

It is the diameter ratio of orifice hole (D_h) to pipe diameter (D_p). It is also known as Equivalent diameter ratio (EDR)

$$\beta = \left(\frac{D_h}{D_p} \right) \tag{2.11}$$
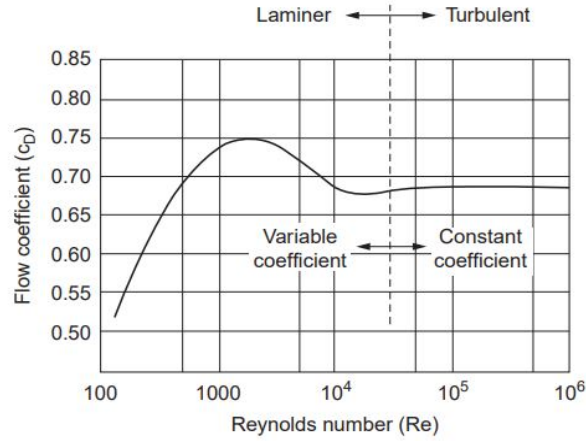
Figure 2.10: Flow regime effects on the discharge coefficient of a flow nozzle [Altendorf, 2006].

Discharge coefficient

In a single-phase flow the discharge coefficient is mainly dependent on Porosity (β) and Reynolds number. It represents the ratio of actual to theoretical flow rate.

$$C_d = \frac{Q_{actual}}{Q_p} \tag{2.12}$$

It is modelled that discharge coefficients are very close to unity for Venturi and nozzle flow meters [Campos et al., 2014]. However, in orifice meters discharge coefficients are quite less than 1 due to vena contracta effects. Based on Reader-Harris Equation from "ISO 5167 D and D/2 tappings" [Reader-Harris and A, 1996]the discharge coefficient can be described as

$$\begin{aligned} C_D =& 0.5959 + 0.0312\beta^{2.1} - 0.184\beta^8 + 0,0029\beta^{2.5} \left(\frac{10^6}{Re_{Dm}}\right)^{0.75} \\ &+ 0.09 \left(\frac{L_1}{D}\right) \left(\frac{\beta^4}{1-\beta^4}\right) - 0.0337 \left(\frac{L_2}{D}\right)\beta^3 \end{aligned} \tag{2.13}$$

Where L1 and L2 are the D and D/2 tapping distances. Re_m is the mixture Reynolds number. A relation between Reynolds number and discharge coefficient is shown in Figure 2.10

2.2.2 Measurement principle

Orifice meter works on the principle of interruption of flow inside a pipe. By employing the Bernoulli equation for friction less flow and measuring a pressure drop across an orifice we can
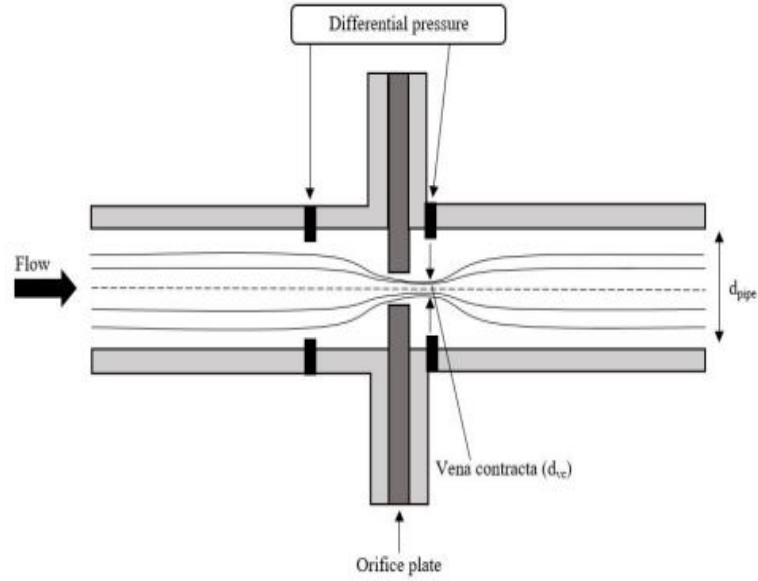
Figure 2.11: Principle of an orifice plate[Hansen et al., 2019]

determine the rate of flow.

The point at which flow experiences maximum amount of convergence is called vena con-
tracta. As shown in Figure 2.11, Vena Contracta occurs just after the orifice plate. A differential
pressure sensor measure the pressure difference or pressure drop across the plate by employing
Bernoulli's equation velocity of the fluid can be obtained.

Let upstream and downstream pressure tapping be P1 and P2, applying Bernoulli's theorem and
continuity equation, an equation for volumetric flow is derived:

$$\frac{P1}{\rho g} + \frac{V_1^2}{2g} = \frac{P2}{\rho g} + \frac{V_2^2}{2g} \tag{2.14}$$

where, V1 and V2 are the velocities at upstream (P1) and downstream (P2) pressure tappings
respectively, ρ is the density of a fluid and g is the gravitational component. From continuity
equation where A1 and A2 are areas of orifice and pipe respectively, We get:

$$V_1 A_2 = V_2 A_1 \tag{2.15}$$

From Eq. 2.14 and Eq. 2.15,

$$V_2 = \sqrt{\frac{2(P1 - P2)}{\rho \left(1 - \frac{A_2^2}{A_1^2}\right)}}$$

Volumetric flow rate is given by,

$$Q = A_2 V_2$$

Substituting gives us ,

$$Q = \frac{A_2}{\sqrt{1 - \beta^4}} \sqrt{\frac{2(P1 - P2)}{\rho}} \qquad (2.16)$$

However, Eq. 2.16 applies only to perfectly laminar, inviscid flows. To account for the effect of viscosity and turbulence that convert kinetic energy into heat, a discharge coefficient, C_d is introduced, which marginally affects the flow rate Q.

$$Q = \frac{A_2 C_d}{\sqrt{1 - \beta^4}} \sqrt{\frac{2(P1 - P2)}{\rho}} \qquad (2.17)$$

where $\beta = \sqrt{\frac{nA_2}{A_1}}$, the ratio of the square root of total orifice open area to pipe area, (n - Number of holes).

For a two-phase flow orifice meter flow equation [Fadaei et al., 2021] is represented below:

$$Q_t = \frac{C_D}{\sqrt{1 - \beta^4}} {}^* \xi^* \pi / 4^* d^{2*} \sqrt{2^* \rho_m {}^* \Delta p} \qquad (2.18)$$

where Q_t is the two-phase mass flow rate. A detailed explanation of Equation 2.18 is given in Appendix B.

2.2.3   Studies on multiphase pressure drop in orifice meters

Studies related to measurement of flow rate and quality of vapor-liquid mixture have been interest of many fields. An orifice, being a cheap, convenient and reliable device, has been a focus of research for several decades. For instance, air-water studies[G. G. and McFarlane, 1967][Chisholm, 1967] and steam-water tests [Collins and Gacesa, 1971],[Chen et al., 1986] have been a primal focus.

Various theoretical models have been proposed for two phase flow through orifice. For an incompressible flow, pressure drop across orifice is comparatively small when compared to total pressure drop. However, in compressible conditions, (i.e. actual conditions in process industry)

pressure drop is much higher and modelling compressible flow is quite a challenge [Lis, 1982]. In order to estimate the pressure drop under two-phase conditions, a correction factor is applied to the single-phase pressure drop. Here, a dimensionless number, Φ_{LO}^2, relates the two-phase pressure drop Δp_{TP}, to the pressure drop if only liquid was flowing Δp_{LO} .

$$\Phi_{\text{LO}}^2 = \Delta p_{\text{TP}}/\Delta p_{\text{LO}} \tag{2.19}$$

Two-phase models

Genereally two-phase models can be subdivided into two categories:

- Homogeneous flow model [Wallis, 1969]

- Separated flow models

Homogeneous model

If the two phases were homogeneous, meaning, the liquid and gas flowing at the same velocity ($Slip = 1$), then it would behave as a single phase flow [Wallis, 1969]. It is expressed by:

$$\Phi_{\text{LO}}^2 = 1 + x \left[\frac{\rho_l}{\rho_g} - 1 \right] \tag{2.20}$$

Where, x is mass flow quality. This concept is visualised using a homogeniser [Falcone, 2009] but has not been practically demonstrated with accurate measurements .

Separated Flow

Several two-phase models have been developed to express the phase pressure drop multiplier. Some of them are listed below:

The Lockhart and Martinelli Model 1949

Assuming the seperated two phase flow and using Lockhart Martinelli approach [Lockhart and Martinelli, 1949], the pressure drop multiplier can be expressed as:

$$\Phi_{Lo}^2 = 1 + \frac{CL}{X_P} + \frac{1}{X_P^2} \tag{2.21}$$

where the value of C_l depends on the slip and flow regime. The Lockhart Martinelli parameter X_P is expressed is defined as:

$$X_P^2 = \frac{(dp/dz)_L}{(dp/dz)_G}$$

where

$$\left(\frac{dp}{dz}\right)_L = f_L \frac{2G^2(1-x)^2}{D\rho_L}$$

$$\left(\frac{dp}{dz}\right)_G = f_G \frac{2G^2 x^2}{D\rho_G}$$

where,

- f = phase friction factor,

- ρ = phase density,

- x = gas quality

- G = total mass flux

- D = pipe diameter

The Simpson Model [Simpson et al., 1981]

The pressure drop multiplier can be expressed as:

$$\Phi_{LO}^2 = [1 + x(S - 1)]\left[1 + x\left(S^5 - 1\right)\right]; \quad S = \left(\frac{\rho_l}{\rho_g}\right)^y \tag{2.22}$$

The exponent y ranges from 0 to 0.5 for no-slip to maximum slip. A value of 1/6 was proposed by [Simpson et al., 1981] through experimental correlations.

The Chisholm Model (1983)

Chisholm [Chisholm, 1983] developed the following equation for two-phase frictional pressure drop:

$$\Phi_{LO}^2 = 1 + \left(\frac{\rho_l}{\rho_g} - 1\right)\left[Bx(1 - x) + x^2\right] \tag{2.23}$$

Here, B is a factor involving slip ratio, flow area and the contraction coefficient (C_c), for thick and thin orifice plates shown in Figure 2.12 . It can be expressed as below:

Thin orifice

$$B = \frac{\left[\frac{1}{(C_c\beta)^2} - 1\right]\frac{1}{S} - \frac{2}{C_c\beta S} + \frac{2}{S^{0.28}}}{\frac{1}{(C_c\beta)^2} - 1 - \frac{2}{C_c\beta} + 2}$$

Thick orifice

$$B = \frac{\left[\frac{1}{(C_c\beta)^2} - 1\right]\frac{1}{S} - \frac{2}{C_c\beta^2 S} + \frac{2}{\beta^2 S^{0.28}} - \left[\frac{1}{\beta} - 1\right]\frac{2}{S^{0.28}}}{\frac{1}{(C_c\beta)^2} - 1 - \frac{2}{C_c\beta^2} + \frac{2}{\beta^2} - \frac{2}{\beta} + 2}$$

where Compaction coefficient is

$$C_c = \frac{1}{[0.639(1 - \beta)^{0.5} + 1]}$$

Slip can be calculated from: $S = \left\{ \begin{array}{ll} \left(1 + x\left(\frac{\rho_l}{\rho_g} - 1\right)\right)^{0.5} & \text{if} \quad X > 1 \\ \left(\frac{\rho_l}{\rho_g}\right)^{\frac{1}{4}} & \end{array} \right\}$

and the LockHart Martinelli two phase multiplier X is

$$X = \frac{(1 - x)}{x}\left(\frac{\rho_l}{\rho_g}\right)^{0.25}$$
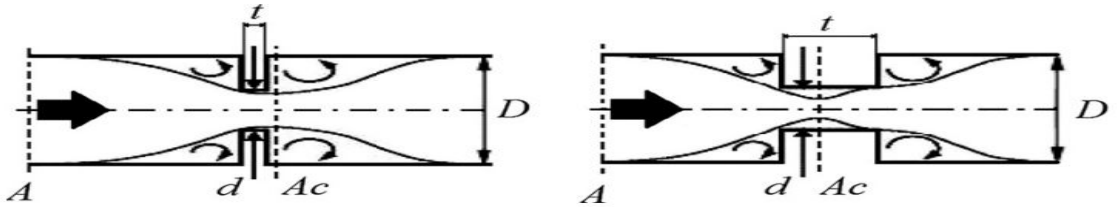
Figure 2.12: Thin and thick orifice[Zeghloul et al., 2017]

The Morris Model (1985)

S.D. Morris Developed a model [Morris, 1985] similar to Chisholm, however, it was much accurate for thin orifice plates when compared to Chisholm [Zeghloul et al., 2017]. The pressure drop multiplier can be expressed as:

$$\Phi_{\text{LO}}^2 = \left[x\frac{\rho_l}{\rho_g} + S(1 - x)\right]\left[x + \left(\frac{1 - x}{S}\right)\left(1 + \frac{(S - 1)^2}{(\rho_l/\rho_g)^{0.5} - 1}\right)\right] \tag{2.24}$$

The slip is calculated similar to that of Chisholm.

An assessment from Zeghloul et. al revealed that the most reliable pressure drop relationships

are from Morris[Morris, 1985] and Simpson [Simpson et al., 1981]. Consequently, conventional correlations are not suitable to represent multiphase pressure drop multiplier and modifications to the models are constantly required. This is due to significant effects of geometry on the fluid dynamics through an orifice (also Multiple orifce Valve (MOV)).

2.2.4 Bubble Cavitation

Cavitation is a general phenomenon that occurs when liquids are transported in pipelines. In order for cavitation to occur, a sufficient reduction in static pressure is necessary [Yan and Thorpe, 1990]. This could be achieved by a restriction, such as an orifice. It is vital to predict cavitation since it plays a crucial part in understanding the flow patterns before and after a restriction. Velocity and pressure profiles across an orifice are shown in Figure 2.13. At the minimum flowing area (vena contracta), the velocity is at its maximum, using the continuity equation 2.14. Consequently, the static pressure is at its minimum. This reduction in static pressure initiates the growth of bubble cavities. The pressure recovery ahead of vena-contracta causes collapse in cavitation [Yan and Thorpe, 1990]. In some cases super cavitation occurs and the general flow after the orifice is annular jet flow.
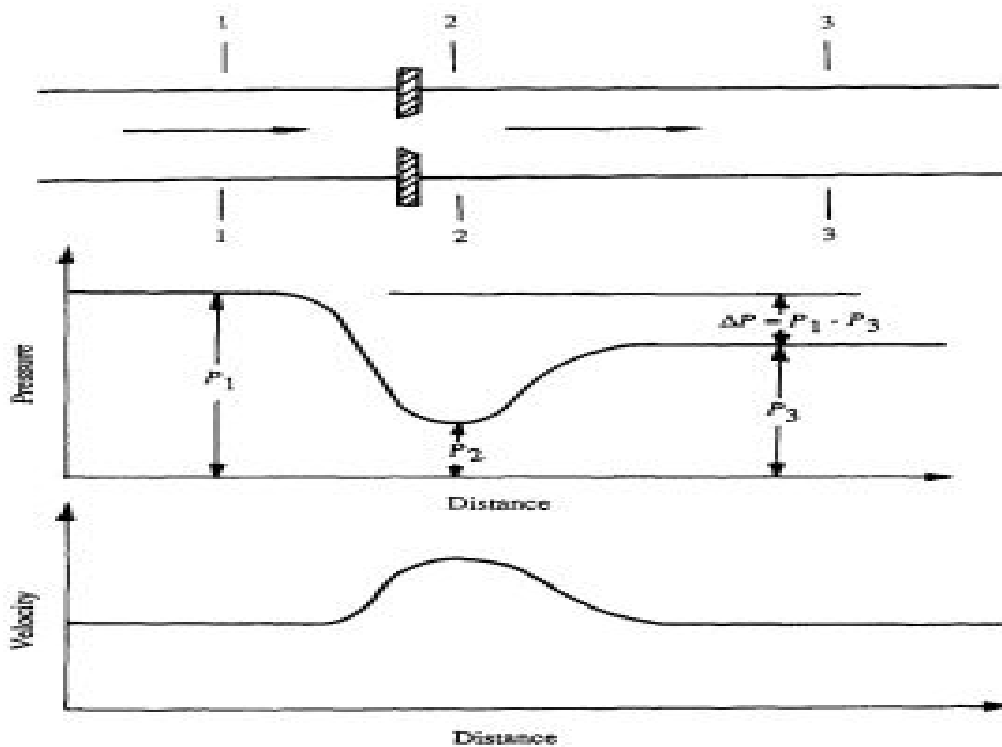
Figure 2.13: Pressure and Velocity profile across orifice [Yan and Thorpe, 1990]

Cavitation inception

A dimensionless number known as cavitation number is widely used to study cavitation inception. It is represented below:

$$\sigma = \frac{P_3 - P_v}{\frac{1}{2}\rho V^2} \qquad (2.25)$$

Where P_3 is the downstream pressure, P_v is the vapor pressure of water, and V is the liquid velocity at the orifice. The experiments conducted by Yan et al. [Yan and Thorpe, 1990] conclude that cavitation inception, i.e., flow transition from single-phase to two-phase bubbly flow, is independent of liquid velocities. As shown in Figure 2.14, cavitation number is linearly related to β (the diameter ratio) and has a strong size scale effect. As compared by Yan et al., the cavitation number changes with a change in pipe sizes. Hence, there is a release of gas bubbles when pressure changes significantly.
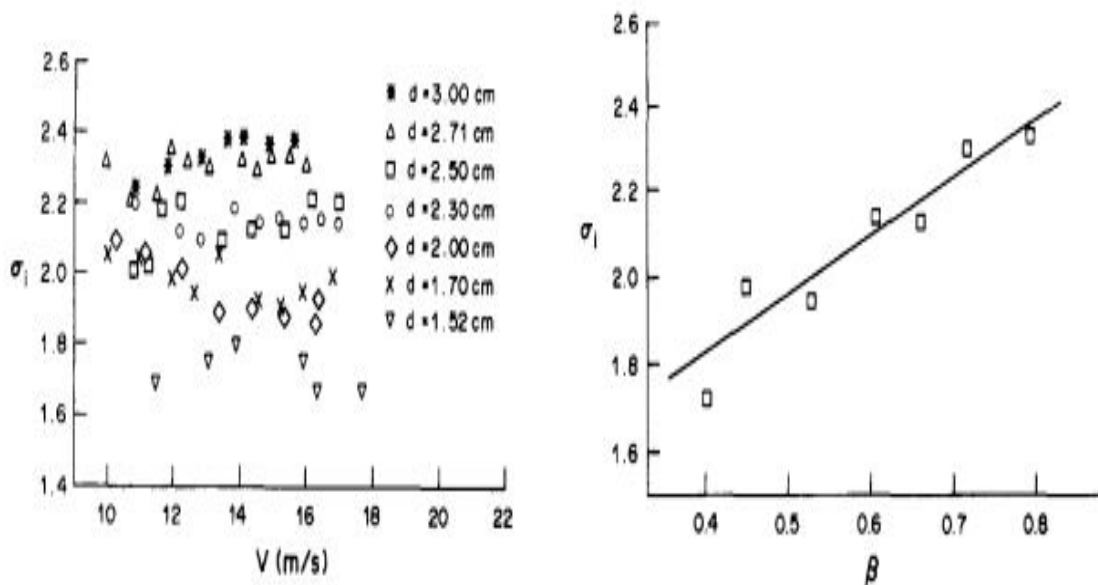
Figure 2.14: left: Cavitation number σ vs liquid Velocity (V) for seven orifices. Right: Cavitation inception number (σ) vs the diameter ratio (β) [Yan and Thorpe, 1990]

Super-Cavitation

Towards the downstream of orifice, super-cavitation tends to occur. Yan et al describes the following regions:

- Region A - Annular jet flow in middle of air pockets.

- Region B - Mixing zone where cavity breaks into smaller cavities (this zone is relatively small compared to region A).

- Region C - Clear region where only liquid is present and bubbles disappear.

Figure illustrates the different regions present. The sizes of these regions depend heavily on orifice geometry as well as the flow rates and pressure drops across the region [Yan et al., 1988].
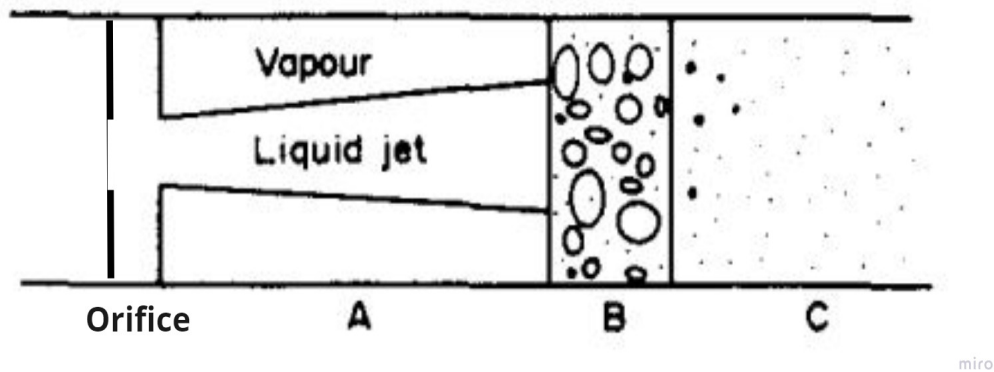
Figure 2.15: Super Cavitation [Yan and Thorpe, 1990]

2.3   Summary

From the literature covered, it can be established that several factors influence multi-phase flow through an orifice. Some of them are:

- Type of flow entering the orifice. The flow regime in which the incoming fluid enter the orifice affect Reynolds Number and pressure losses.

- The porosity β is one of the deciding factors affecting flow regime transition and pressure readings.

- Several other factors including thickness of orifice, pipe dimensions and densities of fluid also affect pressure losses.

In addition, several pressure drop models for multi-phase flow were discussed, covering significant geometric parameter to quantify pressure drops through orifice.

A phenomenon of sudden single-phase conversion to multi-phase flow due to cavitation has also been discussed. This could further be evaluated while experimenting as to whether it is dissolved gas that is evolving from water or is water vaporizing when a sudden change in velocities and pressures occurs.

Chapter 3

Research Methodology

Two phase flow through orifice in pipelines are a major source of disturbances and the aim of this research work is to aid understanding of multiphase flow through orifice. Orifice meters are handy, and to replicate such meters cheaply with use of readily available materials in the multiphase laboratory at University of Stavanger has been the focal point of this Master's Thesis. The parameters of interest are outlined first. The sections that follow highlight the approaches taken to address and measure the variables mentioned.

3.1 Variables of interest

- **Pressure drop**

  It is important to measure this variable during analysis. As discussed in the previous Chapter, pressure losses occur whenever fluid passes through orifice. It can be affected by orifice geometry and incoming fluid conditions.

- **Pressure Changes/Fluctuations**

  In order to quantify disturbances in flow, analysis of frequency spectral will help in understanding the flow mechanisms present. For example, pressure fluctuations tend to change with a change in the flow rate of the fluids present.

- **Mass Flow rates**

  Measuring flow, either liquid or gas, is a critical variable in many processes. It is vital to

know the amount of fluid present in a given place at a given time. Often, flow meters are combined with pressure and temperature values to measure mass flow.

3.2 Approach

This thesis describes the analysis of Air-water flow through orifices in pipes. Given the low Mach number (M), that is, the ratio of fluid velocity and velocity of sound in that fluid [Labidi, 2019], the flow can be considered incompressible. In addition, present study focuses on non-cavitating flow with low gas rates (bubbly or plug flows).

From section 3.1, the mentioned variables can be determined through experiments or numerically. By adopting an experimental approach to the problem the measurement of parameters of interest was done through setups and available equipment.

- **Pressure Drop Measurement**

  This involves measuring the pressure drop and fluctuations across the orifice. Considering the approaches in earlier experiments [Qing et al., 2006] and resources available in the present flow loop, the pressure readings are measured directly using differential pressure sensor. This approach is detailed in Chapter 4 and the results discussed in Chapter 5.

- **Flow rates and flow mechanisms**

  The flow rate of fluids (air and water) upstream of the orifices has been evaluated using available flow rate sensors (magnetic and vortex sensors). Flow mechanisms are identified using visual observations and video footage. Chapter 4 further describes the complete flow loop and flow rate measuring instruments in detail.

The measurements taken are meant to identify flow structures and mechanisms occurring downstream of the orifice. Furthermore, the generated experimental data can be utilized and projected on CFD analysis commonly used in the industries.

It is required to gather experimental data quickly. Thus, a pipe with an orifice fitting was built to make changing the orifice much faster. In addition, it could also be removed and replaced on the rig at any time necessary.

3.3   Research Questions

The present experimental investigations aim to answer some of the below-mentioned research questions:

- How reliable is an orifice in metering two-phase (air-water flow). Can we use a single or multi-hole orifice to differentiate the flow mechanisms?

- Comparing effects (from pressure drop ratings) on different orifices. Do geometrical parameters affect the magnitude of flow mechanisms, and to what extent?

- Does flow disturbance have any relation with external parameters?

- Is this method applicable to industrial flow systems? Can we accurately measure and evaluate flow conditions inside the pipe?

From the Literature review in Chapter 2, it can be understood that many models and experimental investigations have analyzed two-phase flow through an orifice. By measuring pressure differences across the orifice and visual observations using several geometries, this study aims to utilize the flow rig at the University of Stavanger.

Although the pressure fluctuations range is much lower than actual industrial processes, it is a step forward in developing a cheap orifice meter in the lab. It is believed that the results attained in this experiment will further add to an understanding of multiphase flow through the orifice.

The experiments can be further validated using CFD simulations. To the author's knowledge, no previous experimental setups have been carried out at the University of Stavanger involving two-phase flow through an orifice. This could perhaps be related to the complex nature of the multiphase flow.

3.4   Summary

This Chapter outlines the research methodology that was used in this study. Some research questions have been discussed. And the approach taken to measure the parameters has been mentioned. Subsequent Chapter describes experimental setup in detail.

Chapter 4

Experimental Setup

4.1   Introduction

This Chapter provides a detailed description of the experimental procedures carried out in multiphase flow loop. The components of the loop have been discussed in detail. Furthermore, the test section containing Orifice and pressure drop sensor has also been described. Orifice setup and geometries are part of the experimental procedures carried out in the lab.

4.2   Flow loop

The components of the flow loop on which the test section was set up are shown in Figure 4.1. The subsequent sections begin with a setup overview and a detailed description of the experimental apparatus used.

4.2.1   Setup Overview

A continuous flow of water-air mixture by pumps is channeled into the test section using connecting hoses. The fluid passes through an orifice plate. The positioning of sensors is upstream and downstream of the orifice. Signals from transducers are recorded using a data-acquisition system. The flow is channeled back to the pump reservoir using connecting hose pipes from the test section. A flow meter and differential pressure sensor measure the flow rates (water and air
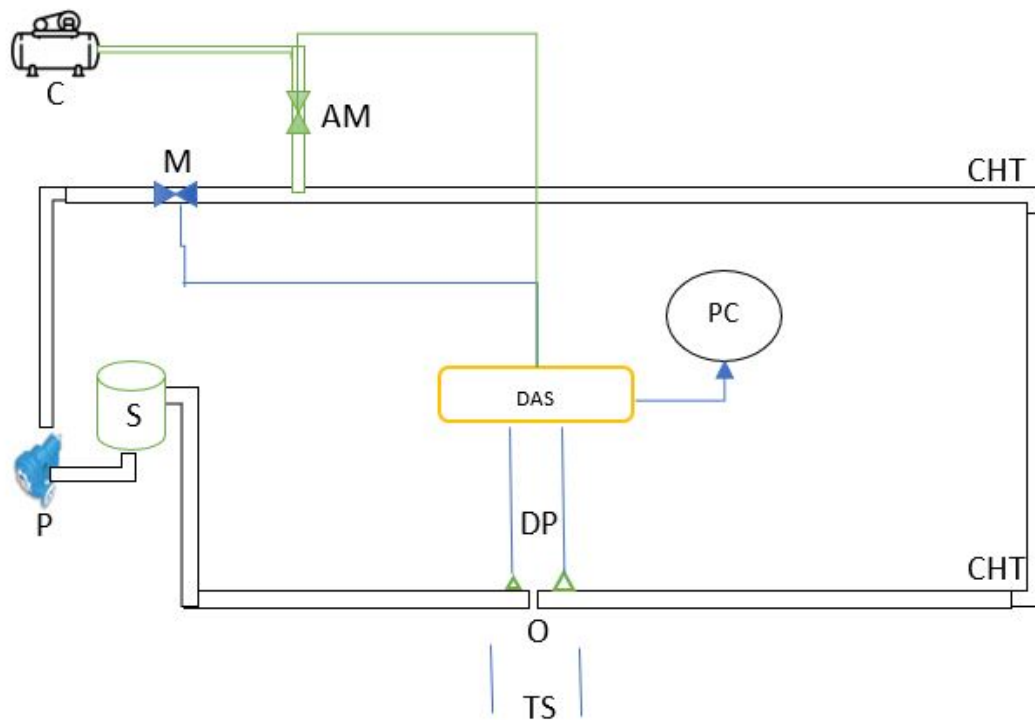
Figure 4.1: Schematic of flow loop for pressure measurement.

separately) and the pressure difference.

4.2.2   Instrumentation and arrangements

- **Water tank and Separator**

  A water tank made of Plexiglass with a capacity of two hundred Liters supplies de-ionized

  water to the flow rig. It also acts as a separator when the fluids are pumped back into it. A

  swirl at the top is observed as the water gets poured back, making it a closed loop. Figure

4.2 displays the separator tank.

Figure 4.2: Separator and Water tank

- **Pump**

  Multi-stage progressive cavity pump is used that supplies water. A PCM 25I5 pump with a maximum pumping rate of $12m^3/h$ is used. An electronic-flow-control valve, part of the Pump, is used to control the flow rate. The Pump was running at 10, 15, 20, and 25 percent capacity for the experiments.

  Air is supplied through a compressor, and a mass flow controller regulates the airflow. Air is supplied to the flow rig from the top.

- **Connections**

  Flexible hoses made of polyurethane connect the Pump to the flow rig. Several acrylic pipes are connected that complete the rig. The rig consists of two horizontal elbows, and a straight section of length $6.7m$ connects to the flow rig's test section (orifice section). Most of the parts of the rig are transparent so that the flow mechanisms can be visualized.

- **Differential pressure sensor**

  A digital differential pressure, $Rosemount 3051CD3A$ is connected onto the pressure tappings, upstream and downstream of the orifice. Table 4.1 outline the specifications of the sensor.

  It determines the steady or fluctuating pressure difference between the orifice. The pressure tapping distances are further discussed in Orifice meter setup for the experiment.

Property	Value
Measurement range	-2480 to $2480\ mbar$
Transmitter output	$4 - 20mA$ HART protocol
Accuracy	0.04% of span
Response time	100ms

  Table 4.1: Specification of Rosemount 3051CD3A differential pressure sensor as reported by manufacturer

- **Magnetic flow meter**

  A magnetic flow meter, ABB MAGMASTER MFE200, is used to measure the volumetric flow rate of water inside the loop. The magnetic flow meter works on the principle of Faraday's Law of induction. It is compromised of a sensor and a transmitter that detect flow. The sensor measures voltage generated by fluid as it is flowing through the magnetic field. This voltage is converted to flow measurement by the transmitter and sent to a control/data acquisition system. The figure below shows the Magnetic flow meter in the flow loop.

Figure 4.3: Magnetic Flow Meter

- **Mass flow controller**

  A mass flow controller to regulate the inflow of air is used. ALICAT MC-10SLPM is the installed flow controller with setpoints ranging from 0 to 10 SLPM (Standard liters per minute). Table 4.2 lists the specification of the flow controller.

Property	Value
Operating temperature range	$-10°C$ to $+60°C$
Full scale operating pressure	160 psia
Set point range	0 to 10 SLPM
Accuracy	0.6% of reading
Repeatability	0.1% of reading $+$ 0.02% of full scale
Response time	30ms
Fluid	Air

  Table 4.2: Specification of ALICAT MC10SLPM mass flow controller

- **Data acquisition system and software**

  All sensor data is sampled and collected in data acquisition system and is controlled using LABVIEW SOFTWARE.

- **Test Section**

  The flow reaches the test section through connecting tubes. The internal diameter of the test section is 40mm, and the total length is 67 cm. The test section is connected using hard-plastic connectors. The weight of the test section is around 1.8 kg. As seen in figure 4.3, the test section contains an orifice ring on which the orifice plate settles when pushed down from the upstream side of the pipe. The test sections contain two drilled pressure tappings at distances D and D/2 upstream and downstream of the orifice plate. A rounded acrylic sheet of thickness 10mm is glued on top of the tapping to enable connection with the pressure sensor. Figure 4.4 shows further details.
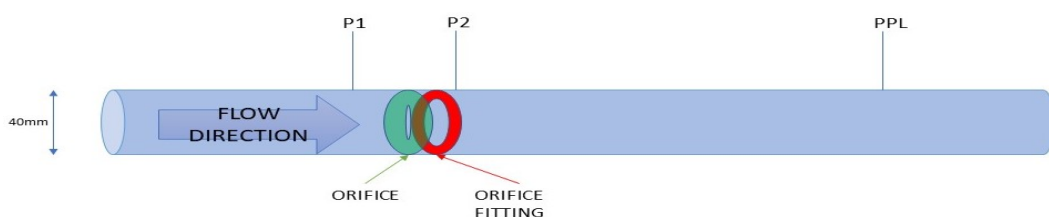

Figure 4.4: Schematic of Test section.

4.3   Orifice Geometries

The current experiment aims to visualize working of orifice plates when air-water flow passes through. The orifices plates used in this experiment are both single hole and multi-hole. This section lists down the types of orifice plates used, as well as how the overall manufacturing of test section was done.

4.3.1   Orifice plates design

Table categorizes the orifice plates used in the experiments. These orifice plates produced a range of pressure losses with different flow rates [Campos et al., 2014]. These orifice plate design considerations are based on ISO-5167-2. All the single hole orifices used are sharp-edged and concentric with the pipe. These plates were designed in AutoDesk Fusion 360. Acrylic sheets of thickness 4mm were laser cut using the Beambox machine available at the University of Stavanger. The Figure 4.5 shows cut out orifices that were placed in the pipe for experimentation.

Plate label	Hole diameter $d_h(mm)$	Plate thickness $t(mm)$	Porosity β	Thickness ratio t/d_h
S1	16	4	0.4	0.25
S2	20	4	0.5	0.2
M1-7hole	7.5	4	0.5	0.525

Table 4.3: Geometries of Single hole (S) and multiple hole (M) orifices

The multi-hole plate was designed so that the geometric variables (β, t) remain constant to single hole. This allows a comparison between the two plates for a similar flow. Furthermore, a few extra plates were also cut out to comply with pipe geometry, and the best fit orifices were chosen.

Figure 4.5: Acrylic Orifice Plates

4.3.2   Pipe design and Pressure Tappings

An acrylic pipe with internal diameter of 40mm was cut and installed in the test section. An acrylic ring of 8mm thickness was placed inside a pipe and tightened in placed using a rubber 0-ring and three screws at 120^0. Following ISO-5167, for pressure tappings, two tappings at distances D and D/2 were drilled upstream and downstream of the orifice sitting. As seen from Figure 4.6 and 4.7 the tappings are shown.
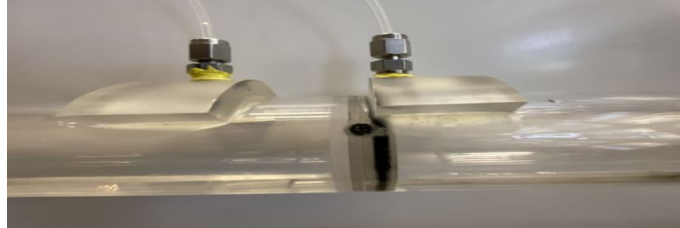
Figure 4.6: Pipe section
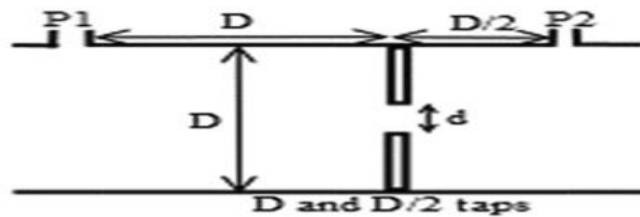
Figure 4.7: D and D/2 taps

4.4   Investigations and Challenges

The setup built for pressure measurements has been described earlier. The aim of these experiments was to visualize the flow patterns occurring when a liquid with small amount of gas is introduced. In addition, a comparison of pressure drops at several flow rates for different geometries is a goal to achieve.

4.4.1   Investigations

Pressure sensor validation

It is essential to ensure that the differential pressure sensor is operating correctly. Furthermore, as the sensor is susceptible, it is crucial to ensure that all the connections are correctly connected

and that the pressure sensor itself is mounted axially to the pipe section.

Its extremely important that pressure tapping were drilled with high accuracy. The Pressure fitting screws were tightened carefully to avoid leaks and ensure accurate readings.

Pump Accuracy

In order to calibrate pump and match the readings on magnetic flow meter a visual experiment was conducted. The outlet was disconnected and flow was diverted to a large bucket, time taken to fill up the bucket at different pump powers was noted. The relation between reading on magnetic flow meter and calculated flow rate is shown in Figure 4.8.

Figure 4.8: Magnetic flow meter vs Calculated Reading

4.4.2   Flow Scenarios

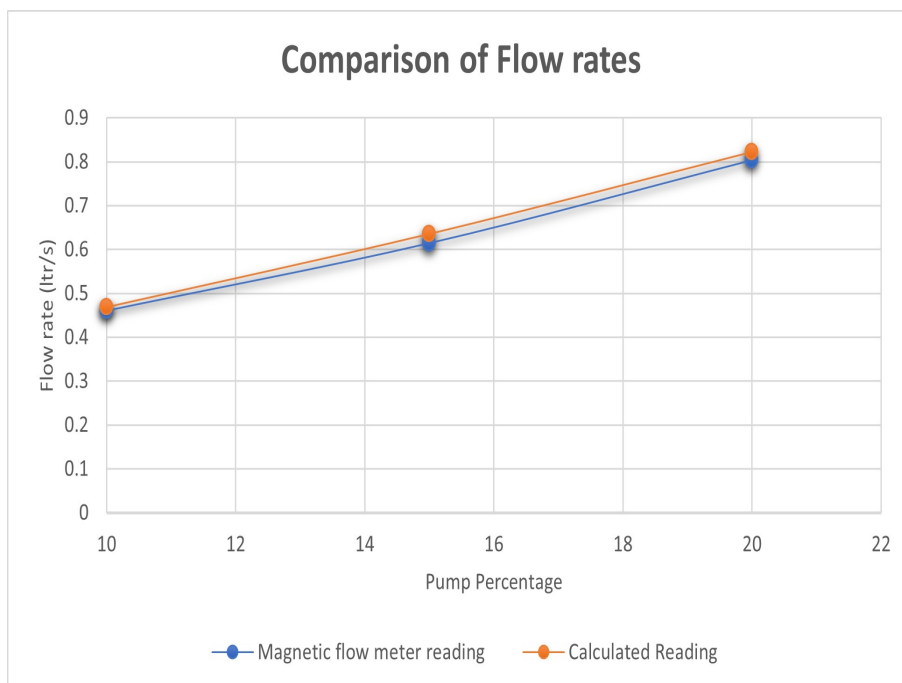The experiments are aimed at studying air-water flow through orifices. Water at 25^0C enters the flow rig and to the test section (orifice). The flow rate was varied between $0.45 - 1 \ ltr/s$ (at pump percentages 10, 15, 20 and 25). Table 4.4 lists the measured and calculated values for water flow rates in the pipe (Dia =40mm).

Pump Percentage	Avg.flow rate(ltr/s)	Superficial Velocities (m/s)	Re_h
10	0.45	0.358	10945
15	0.59	0.469	14338
20	0.77	0.613	18741
25	0.91	0.724	22134

Table 4.4: Water flow rates and calculated Reynolds Number

The increment in the pump rate was kept constant in all the experiments conducted. However, the safest pump power was limited to 20%. At every pump percentage air was introduced in 3 steps. Using mass flow controller to control the air flow and LABVIEW for the input set-point. The air flow rates in standard litres per minute (SLPM) are shown in the table below.

Mass flow rates (SLPM)
1
4
8
10

Table 4.5: Gas mass flow

The flow mechanism observed at the mentioned air-water rates were bubbly and plug flow. This coincides with the mentioned flow patterns in section 2.1.2 and flow regime map [Dukler and Taitel, 1986]. Figure 4.9 shows a flow pattern near orifice.
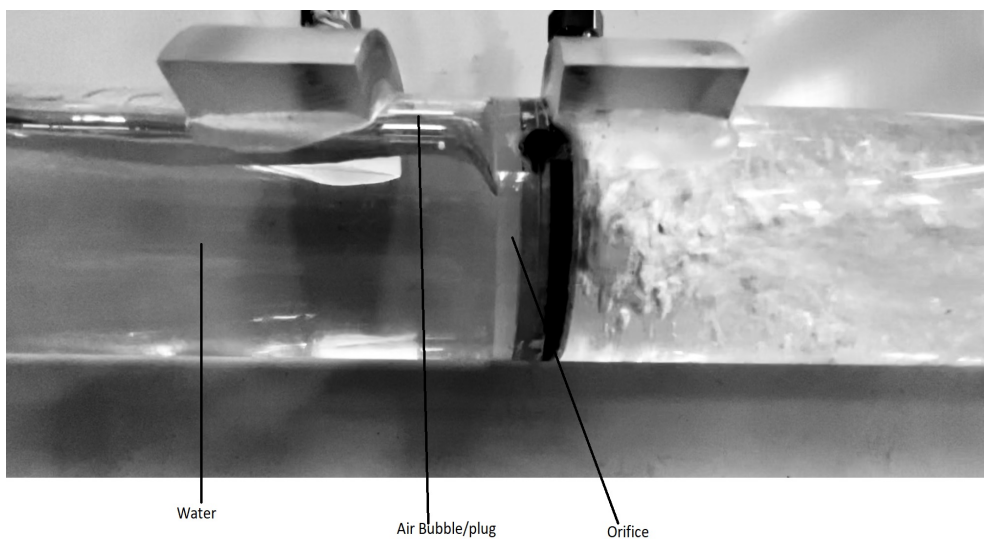

Figure 4.9: Observed flow near orifice

4.4.3 Testing steps

Typical procedures that are followed during testing are:

- 1. The orifice plate is placed inside the testing pipe. The pipe is then connected to the flow loop, and all connections are examined to ensure zero leakage. Finally, the pump is switched on at the lowest rate.

- 2. Before starting data acquisition, the pump can run for 5-10 minutes. First, to ensure no gas/bubbles are present in the system. Next, the orifice's testing section upstream and downstream gets filled with water (Jet is removed).

- 3. Starting with the lowest pump percentage, the air is introduced into the flow rig. At intervals of 100 seconds, the mass flow of air is increased using the set-point in LABVIEW.

- 4. Air is removed from the system after testing for air rates at 1, 4, 8, and 10 SLPM. The pump can run when no noticeable bubbles are observed in the flow.

- 5. The water flow rate is increased (pump percentage is increased), and steps 3 and 4 are repeated.

- 6. At each flow scenario, adequate time is allowed for the rate to establish. The data from LABVIEW is saved and plotted in excel and Python for further investigation. Each orifice plate measurement typically takes 90-100 minutes.

- 7. The water in the setup is allowed to drain, and the next orifice plate is inserted.

4.4.4 Challenges

Some of the challenges faced during experimental setup and investigations include:

- Backflow of water into the air inlet pipes.

  As water flow rates were increased, some back flow of water observed in air inlets. This could be due to the development of back pressure as when air is switched off there is a back pressure that develops. In result, it sucks in the water present in the flow rig.

  This problem was solved but introducing air in very small amount i.e. 1 SLPM.

- Preparation of orifice plates.

  One of the key challenges was to accurately cut orifice plates. An acrylic sheet was used, however, using hand controlled machining tool is a lengthy process. Instead, a laser cutter was used that gave a higher accuracy as well.

4.5 Summary

This chapter discussed the experimental setup and the instrumentation used. Flow loop and orifice geometries has been described in detail. Focus on investigation and challenges was in section 4.4. Chapter 5 is dedicated to interpretation of results and analyzing the flow mechanisms occuring.

Chapter 5

Results and Discussion

5.1 Introduction

The experimental setup and orifice geometries were discussed in the previous chapter. An overview of testing setup was discussed in section 4.4.3.

Results from experimental runs are described in this chapter. The first section illustrates the flow mechanisms observed under different flowing conditions and the subsequent sections analyze pressure fluctuations and pressure losses across orifice. The aim is to understand the effects on pressure losses under different orifice geometries.

5.2 Flow Characteristics

In order to evaluate flow characteristics it is important to note that both sides of the orifice (upstream and downstream) must be completely filled with water. This is to avoid inaccurate readings on the pressure sensor due to atmospheric pressure (pressure from the separator). We begin our evaluation of flow regime changes when optimum pressure drop is achieved at different flow rates and the test section is filled with water as shown in Figure 5.1.
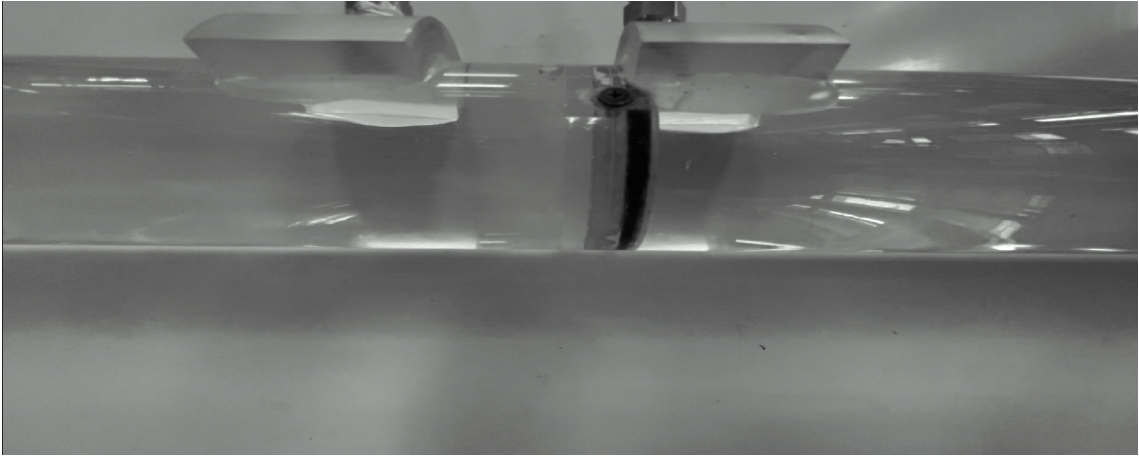
Figure 5.1: Water filled orifice section

5.2.1 Jet Flow

Video recording of the test section was conducted to observe the flow mechanisms visually. Thorough analyses of recorded videos and coinciding parameters were conducted. A jet flow is observed in each experiment. However, the length of the jet varies with varying parameters. Figure 5.2 illustrates the jet flows observed for each orifice plate. It is concluded that the length of the jet would vary with flow rate as well as orifice diameter. At the same flow rates, the longest jet is observed in the orifice with 0.4 β and the shortest with a 7-hole orifice plate.

Figure 5.2: Initial Jet flow at 0.358 m/s Superficial Velocity and No Gas Flow

It is noted that it takes longer for the jet to disappear and the downstream section to be filled with water in 0.4 β orifice than 7-hole. This is due to higher velocities downstream of the orifice as the fluid passes through higher restriction. On the other hand, in 7-hole orifice the multiple jets converge due to Coanda Effect described in section 2.1.4.
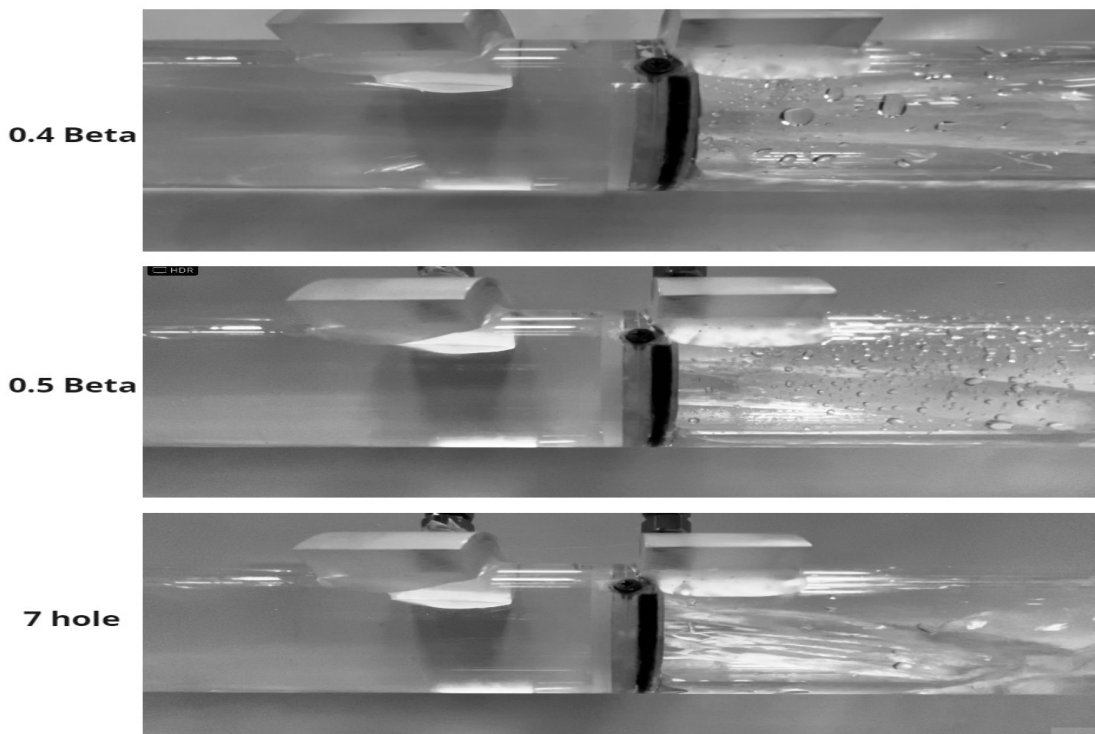
5.2.2 Bubble Observation

In air-water flows random appearance of bubbles is common. These bubbles could be produced by the pump. When passing through orifice, the bubbles are subjected to strong forces and split into smaller bubbles. Observation of bubble behavior through orifices using close-up images was conducted.

The images in Figure reveal an air bubble reaching the orifice and splitting into smaller bubbles downstream. It is observed that the air bubble float on top section of the pipe in Figure 5.3a, due to buoyancy (see section 2.1.2). As soon as it reaches orifice wall it gets sucked through vena-contracta and splits into several smaller bubbles (also can be referred to as cavities in Figure 5.3c).
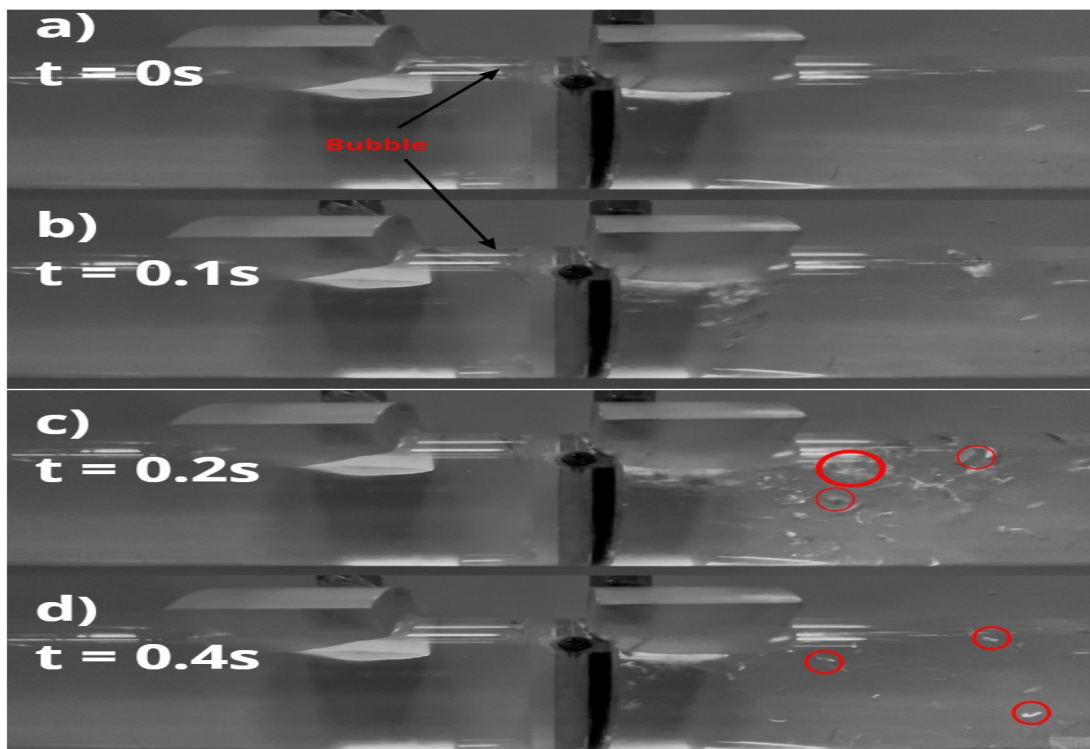
Figure 5.3: Bubble through orifice

5.2.3   Elongated Bubbles and Annular Jets

One of the critical investigations in these experiments was related to elongated bubble flow (plug flow). The Figure 5.4 shows the formation of an annular jet downstream of the orifice when 10 SLPM of air flows at a liquid rate of 0.46 lt/s. It is noted that sudden mixing and separation develops and surrounds the annular jet as both air and water pass through the orifice. A noticeable reduction in pressure drop is also recorded due to the presence of air downstream of the orifice. The lasting duration of these annular jets depend on the size of elongated bubble approaching the orifice. According to studies about cavitation ([Yan et al., 1988], [Yan and Thorpe, 1990]), the regions of downstream flow mechanisms are related to orifice geometries and flow rates.
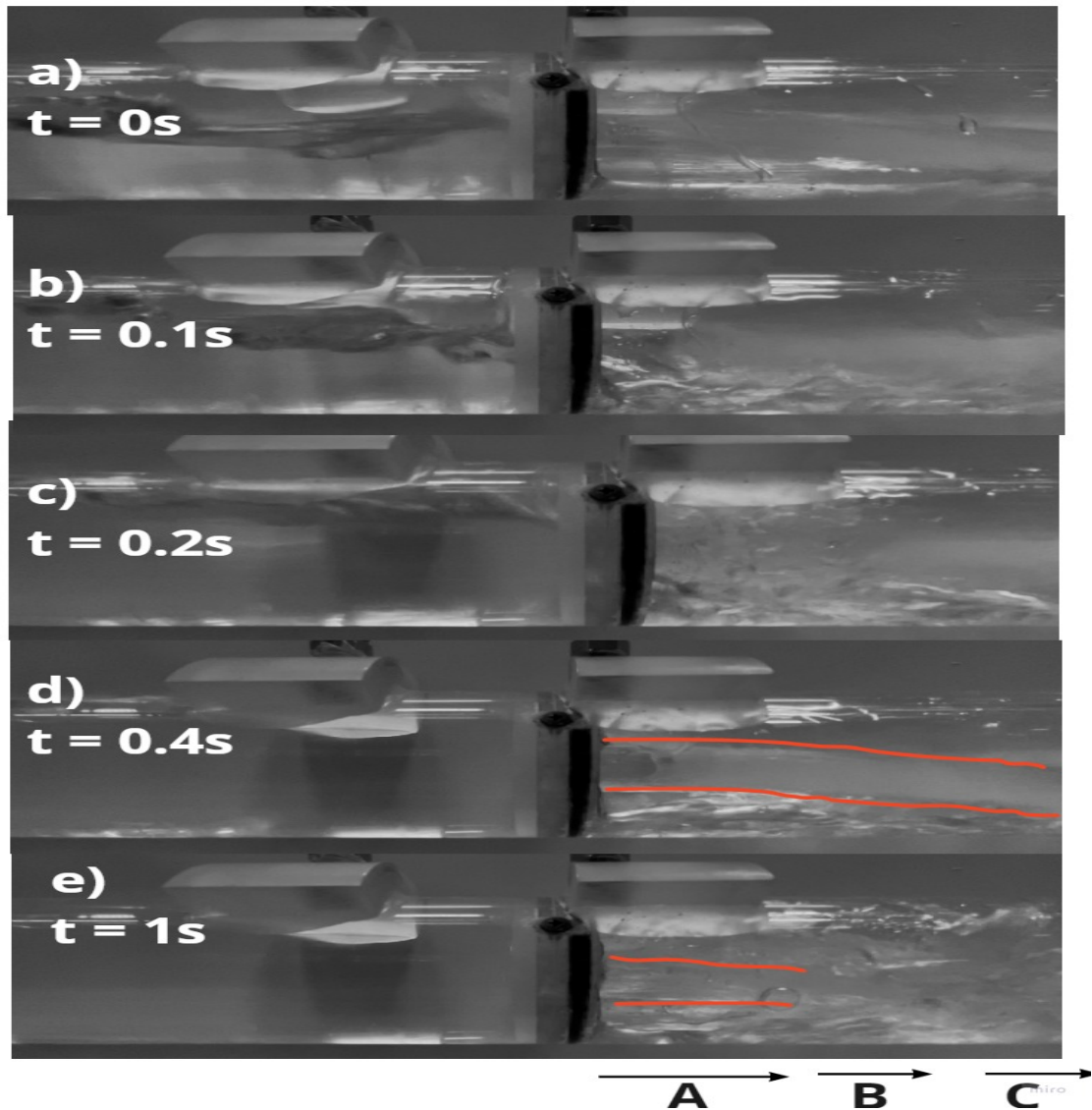
Figure 5.4: Elongated Bubble through orifice at 10SLPM Air and 0.46 Lt/s water

The Flow observed in Figure 5.4 shows similarity to super-cavitation described in section 2.2.4. However, it is merely the separation of air from water. There is a distinct annular jet that typically last for 1 second, and the mixing zones labeled B and C.

In comparison, the observed jet is much smaller in size for a higher liquid flow rate (same gas rate -10SLPM). The mixing and separation are much more violent, and the mixing zones are much closer to the orifice. This vigorous mixing also results in higher pressure drop values and rigorous fluctuations in pressure reading. That will be discussed in the following sections.

Figure 5.5: Elongated Bubble at a high liquid flow rate

5.3 Pressure Measurements

As discussed earlier in section 4.2.2 the pressure readings were taken using a differential pressure sensor. The results from single-phase flow at different superficial velocities of water are shown in Figure 5.6.
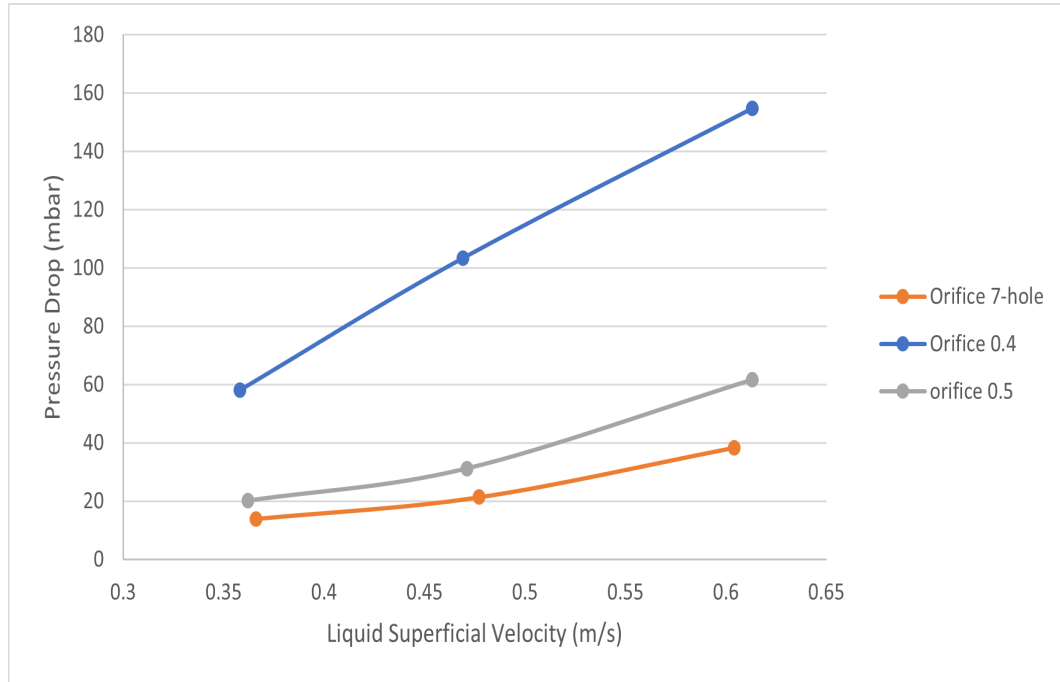
Figure 5.6: Comparison of pressure drops in different orifice plates

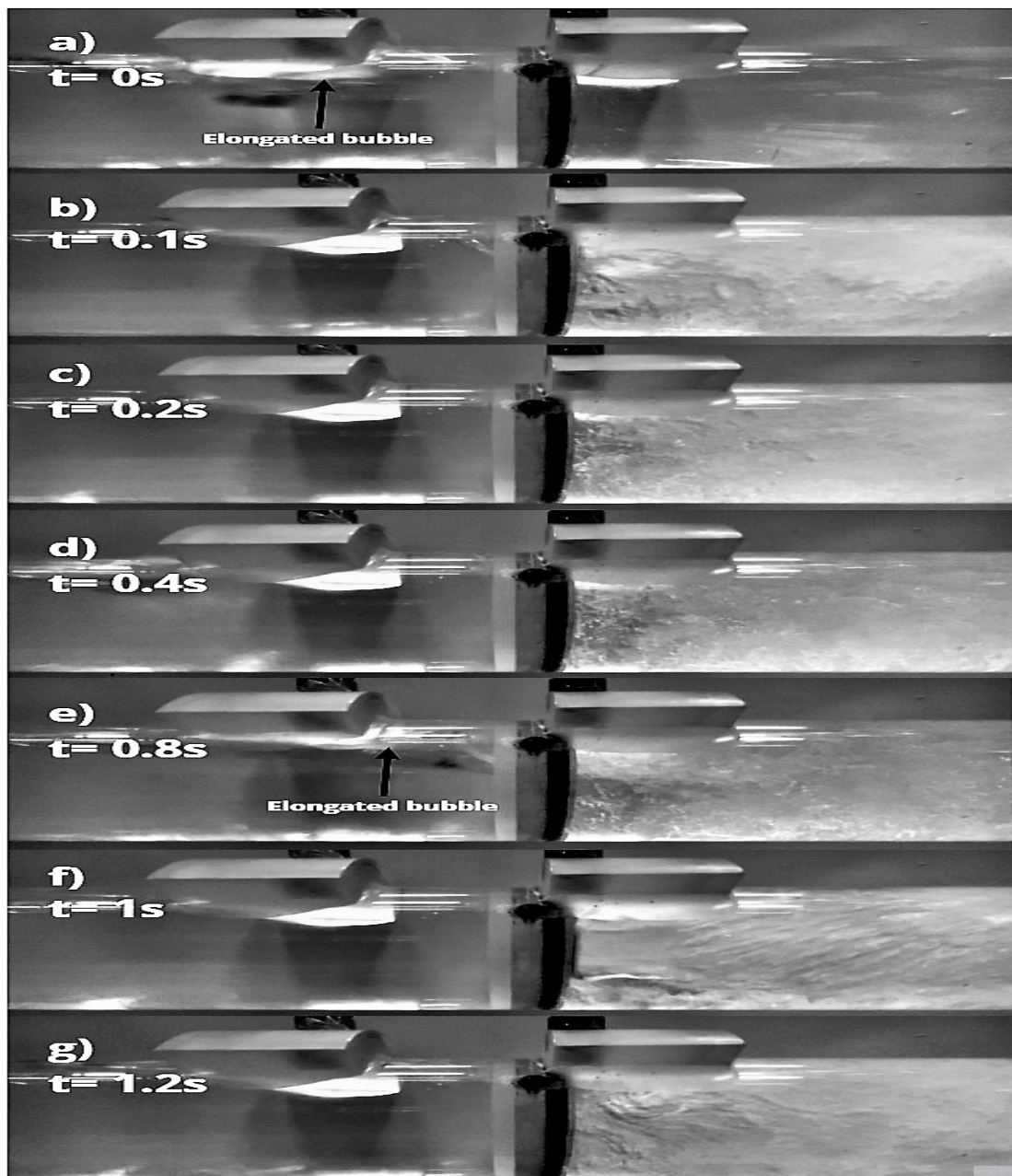It can be deduced that higher the restriction, higher the pressure drop. In case of a multi-hole orifice, the lowest comparable pressure drops are recorded at similar flow velocities.

When comparing the accuracy of orifice during single-phase flow an approach used in ISO standards is applied. That uses the following equation:

$$q_m = \frac{C}{\sqrt{1 - \beta^4}} \epsilon \frac{\pi}{4} d^2 \sqrt{2\rho_1 \Delta p} \tag{5.1}$$

where q_m is the calculated flow rate and ϵ is the expansibility factor (equals to 1 for liquid). Calculations were carried out using an excel workbook (further details in Appendix) The comparison for calculated flow rates and flow rates from magnetic flow meter is made in the table 5.1.

The accuracy of the orifice meter for calculating flow rates when compared to the magnetic flow

Orifice Plate	β (porosity)	Average Pressure Drop (mbar)	Calculated Flow Rate (lt/s)	Magnetic flow meter (lt/s)	Difference %
S1	0.4	58.01	0.450	0.461	2.38
S1	0.4	103.31	0.601	0.598	0.49
S1	0.4	154.78	0.735	0.714	2.86
S2	0.5	20.18	0.456	0.462	1.29
S2	0.5	31.24	0.567	0.595	4.71
S2	0.5	61.63	0.739	0.704	4.73
M1	0.5	13.92	0.459	0.463	1.51
S1	0.5	21.37	0.569	0.591	3.72
S1	0.5	38.38	0.763	0.719	5.71

Table 5.1: Calculated Flow rate vs Magnetic Flow meter

meter is high. It is noted that the lowest pressure drops are recorded for Multi-hole orifices. This comparison ensures that orifice metering used in the Multiphase lab gives us a good idea of flow rates.

5.3.1   Pressure Fluctuations in Two-phase flow

Once the orifices are introduced in the setup, the pressure loss created by different orifices at different flow rates is noted. There are pressure fluctuations observed in the pressure readings whenever there is airflow. This is due to changing flow mechanisms due to air being introduced.

In order to represent these pressure fluctuations, several graphs have been produced using Python. The purpose of these graphs is to illustrate the effect of two-phase superficial velocities on pressure readings. The Figures 5.7 and 5.8 show pressure fluctuations at increasing flow rates of both air and water for orifices S2 (0.5 β) and M1 (7-hole), respectively.

In order to accurately plot the Pressure vs. Time graphs for several flow velocities, the average sampling time of 0.005 seconds has been selected. As the pressure signals from the pressure sensor are not linear with time, i.e., the time step varies between signals, it was important to interpolate the time values for corresponding pressure signals. This interpolation was achieved using Python Code (reader is referred to Appendix A), and the interpolated values from PYTHON are then plotted. In the Figures 5.7 and 5.8 each graph has a consistent time scale of 100 seconds.

As seen from the graphs in Figure 5.7 the pressure fluctuations are smaller at 4SLPM air than 10 SLPM air. This indicates a higher change in flow rates when higher gas is flowing. As
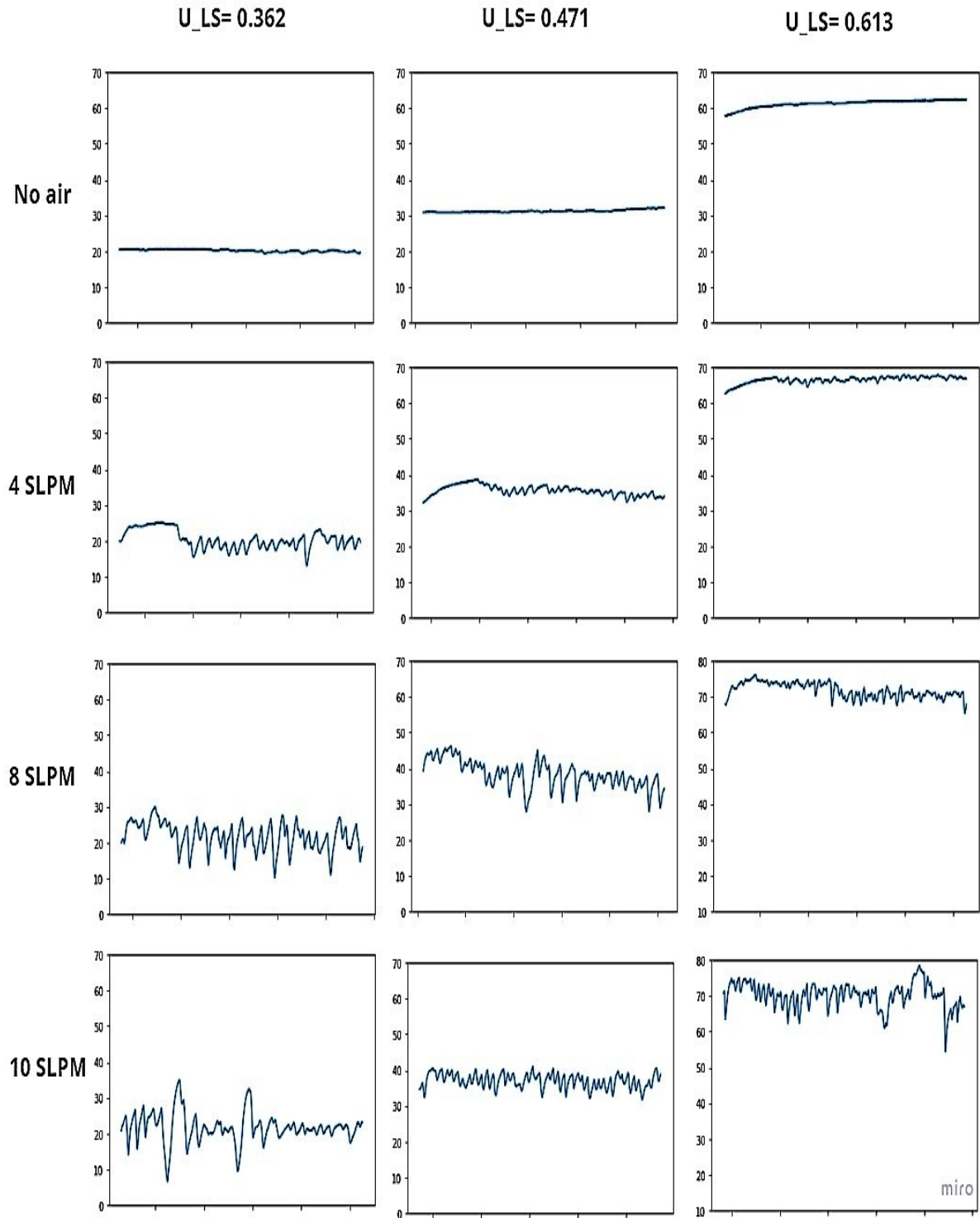
Figure 5.7: Pressure vs. Time for 0.5 β orifice

we know the appearance of elongated bubbles is more common in higher flow rates the pressure drop fluctuation is also higher. A higher change in pressure drops correlates with a longer bubble size. Similarly, in Figure 5.8 with 7-hole orifice the pressure drop when compared to single-hole orifice is lower. The pressure fluctuations are also lower as air bubbles pass through

Figure 5.8: Pressure vs. Time for 7 hole Orifice

the orifice. This is again attributed to cavitation development discussed in section 5.2.3

5.3.2   Relation between Pressure Peaks and Gas flow

Pressure fluctuations occur differently at each different flow rate. A minima is created whenever an air bubble passes through the orifice, and a maxima is created when a liquid continuum is created around the orifice. It can be associated with higher pea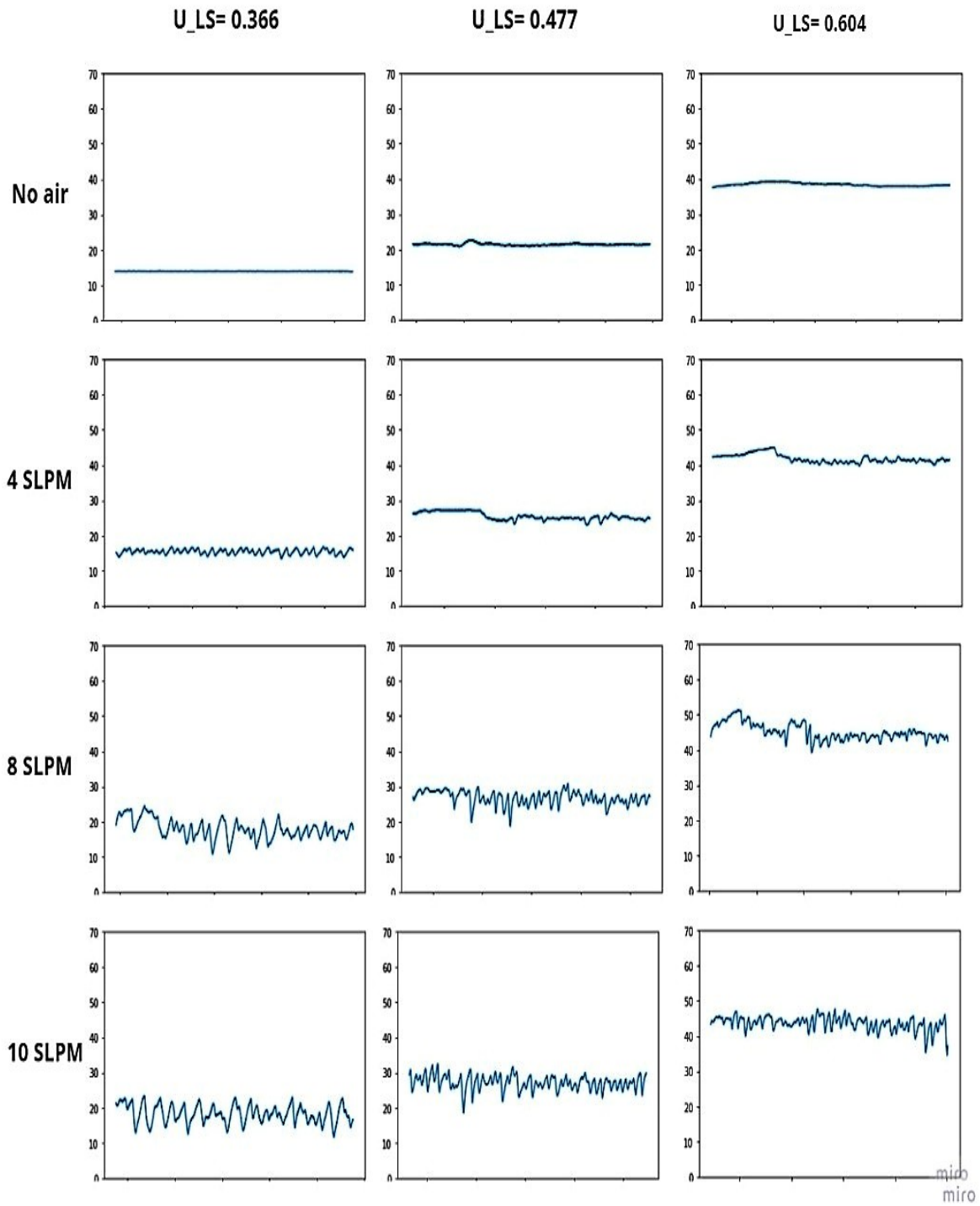ks occurring when jet flow occurs, and the recorded pressure drop is high. On the other hand, a lower pressure drop occurs when downstream becomes liquid-filled, i.e., the bubble has passed through, and jet has stopped.

The constant fluctuation refers to changes in flow mechanisms upstream of the orifice. For example, a lower pressure drop indicates an air bubble upstream of the orifice. This is due to upstream pressure being reduced when an air bubble is present (shown in Figure 5.3), causing a lower pressure drop. Similarly, when only water is present upstream, a higher pressure drop is observed, giving us the idea that the upstream is filled with water. For example for water at superficial velocity $0.362 m/s$ and 10SLPM air, the pressure drops are represented in Figure 5.9. The higher peaks showing liquid filled upstream of orifice and lower peaks showing bubble approaching the orifice.
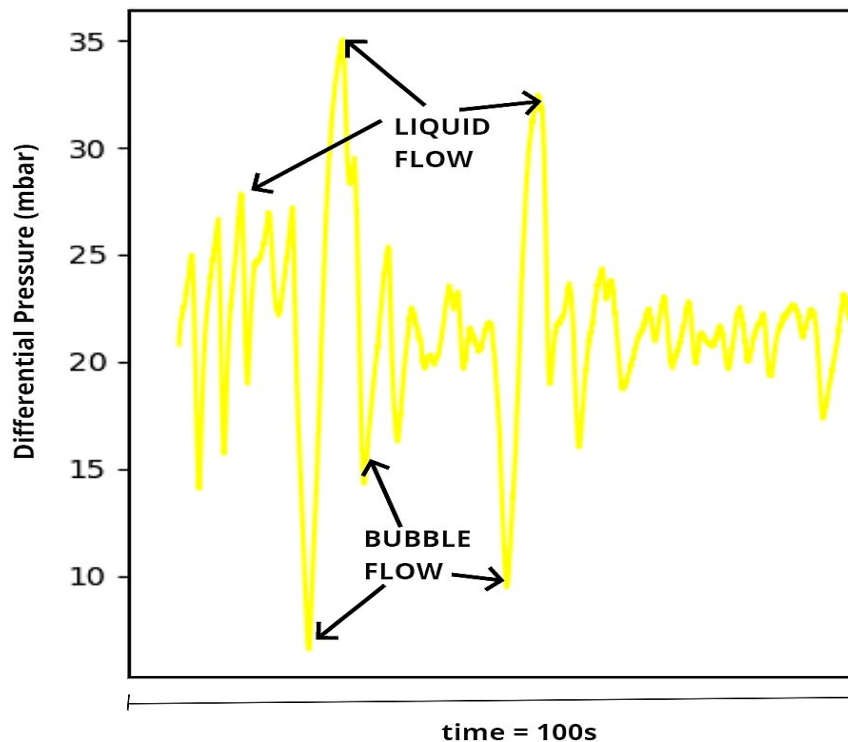

Figure 5.9: Pressure vs Time for 0.5 β Orifice at $U_l s = 0.362 m/s$ and air 10SLPM

An irregular pattern of air bubbles (small bubbles or elongated bubbles) constantly cause a flow rate change that causes a pressure drop change. However, it is possible to analyze the points at which bubbles appear in upstream of the orifice. By using peak analysis in PYTHON the points at which the bubbles are present can be highlighted. A window is chosen at which the peaks occur and the values before and after the peaks are analyzed. The central value gives us the peak, hence, giving us the point at which air bubbles passages through orifice. Figure gives us the peaks for water at superficial velocity $0.362m/s$ and 10SLPM air. The amplitudes of peaks represents the frequency and length of incoming bubbles. Higher the peak, longer the size of the bubbles.Further results are shared in Appendix for separate flow velocities
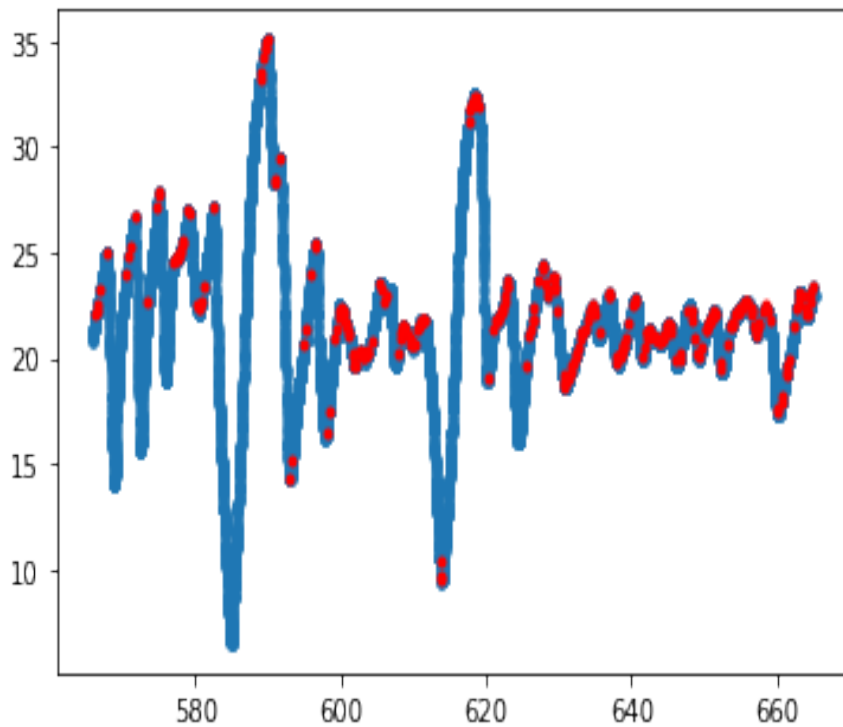
Figure 5.10: Pressure vs Time with peaks for 0.5 β Orifice at $U_l s = 0.362m/s$ and air 10SLPM

5.3.3   Conclusion

The results obtained from pressure measurements and video analysis are presented in this chapter for both single-hole and multi-hole orifices. The effect of flow rates and orifice geometry on flow mechanisms is discussed in detail. The formation of cavities and pressure fluctuations are

discovered to be a factor of airflow.

Comparing a single hole and multi-hole orifice reveals comparable pressure losses. The overall pressure drop and fluctuations are found to be lower in the multi-hole plate. Furthermore, the pressure fluctuations in multi-hole orifices are decaying at a much faster rate when compared to a single hole.

Chapter 6

Conclusion and Scope For Future Work

As concluding remarks, this chapter sums up some conclusions noted in the present experiment. Finally, the author proposes additional work that could further aid in understanding multi-phase flows through orifices.

6.1   Summary of Observations

- A water-air two-phase flow within a horizontal pipe of 40mm Diameter was studied. Multiple orifices that reduces the pipe diameter were laser cut and installed inside the pipe.

- A natural three-dimensional phenomenon of practical relevance supported by experimental and numerical results has been conducted.

- The study contributes to better understanding multiphase characteristics through an orifice inside a pipe.

- The results of this study have demonstrated an ability to visualize flow disturbances across orifice plates with cheaper materials and replicate the industrial process in the multiphase flow lab.

- The turbulent water flows through a sharp-edged single hole orifice in the pipe, resulting in a strong unsteady jet (see section 5.2.3). It is surrounded by large re-circulation regions whose extent is a function of the orifice geometry.

- Despite having significantly different flow features, multiple-hole orifices having the same porosity and thickness can achieve comparable pressure losses.

- Peak fluctuations of pressure were analyzed to represent bubble flows in the pipe. Higher the amplitude of peaks, longer the length of the bubble.

6.2 Further Work

The experimental campaign part of the current project involved large amount of data with still a room for analysis. For instance, the application of correlations stated in the literature ([Morris, 1985],[Chisholm, 1983]) could be a step in revealing additional information about two-phase flow through orifices.

The present study focused on developing an orifice meter cheaply, however, additional experiments at higher gas velocities and several other flow mechanisms could be included, as one of the limiting factors in flow rig are achievable flow regimes.

A numerical validation using CFD studies such as[Fadaei et al., 2021] and [Vemulapalli and Venkata, 2022] could aid understanding of complex nature of flow through orifices. In addition, significant use of test section can be easily conducted for different orifices as they can be cut and placed inside the pipe with not much effort.

References

[Altendorf, 2006] Altendorf (2006). *Flow Handbook, Measurement technologies - applications - solutions*. Endress+Hauser Flowtec AG.

[Barnea, 1987] Barnea, D. (1987). A unified model for predicting flow-pattern transitions for the whole range of pipe inclinations. *International Journal of Multiphase Flow*, 13:1–12.

[Bernoulli, 1738] Bernoulli, D. (1738). *Danielis Bernoulli ... Hydrodynamica, sive de viribus et motibus fluidorum commentarii : opus academicum ab auctore, dum Petropoli ageret, congestum*.

[Brennen, 2005] Brennen, C. E. C. E. (2005). *Fundamentals of multiphase flow*. Cambridge University Press.

[Campos et al., 2014] Campos, S. R., Baliño, J. L., Slobodcicov, I., Filho, D. F., and Paz, E. F. (2014). Orifice plate meter field performance: Formulation and validation in multiphase flow conditions. *Experimental Thermal and Fluid Science*, 58:93–104.

[Chen et al., 1986] Chen, D., Chen, Z., Zhao, Z., and Zhuo, N. (1986). The local resistance of gas-liquid two-phase flow through an orifice. *International Journal of Heat and Fluid Flow*, 7:231–238.

[Chisholm, 1967] Chisholm, D. (1967). Paper 15: Critical conditions during the flow of two-phase mixtures through nozzles. *Proceedings of the Institution of Mechanical Engineers, Conference Proceedings*, 182:145–151.

[Chisholm, 1983] Chisholm, D. (1983). *Two-phase flow in pipelines and heat exchangers*.

[Collins and Gacesa, 1971] Collins, D. B. and Gacesa, M. (1971). Measurement of steam quality in two-phase upflow with venturimeters and orifice plates. *Journal of Basic Engineering*, 93:11–20.

[Dukler and Taitel, 1986] Dukler, A. E. and Taitel, Y. (1986). *Flow Pattern Transitions in Gas-Liquid Systems: Measurement and Modeling*. Springer Berlin Heidelberg.

[Fadaei et al., 2021] Fadaei, M., Ameli, F., and Hashemabadi, S. H. (2021). Investigation on different scenarios of two-phase flow measurement using orifice and coriolis flow meters: Experimental and modeling approaches. *Measurement: Journal of the International Measurement Confederation*, 175.

[Falcone, 2009] Falcone, G. (2009). *Multiphase Flow Metering*, volume 54. Elsevier.

[G. G. and McFarlane, 1967] G. G., Vaughan, V. E. and McFarlane, M. W. W. (1967). Two-phase pressure drop with a sharp-edged orifice.

[Guo and Ghalambor, 2005] Guo, B. and Ghalambor, A. (2005). *Natural Gas Engineering Handbook*. Elsevier.

[Hagedorn and Brown, 1965] Hagedorn, A. R. and Brown, K. E. (1965). Experimental study of pressure gradients occurring during continuous two-phase flow in small-diameter vertical conduits. *Journal of Petroleum Technology*, 17:475–484.

[Hansen et al., 2019] Hansen, L. S., Pedersen, S., and Durdevic, P. (2019). Multi-phase flow metering in offshore oil and gas transportation pipelines: Trends and perspectives. *Sensors (Switzerland)*, 19.

[Kiss and Patziger, 2018] Kiss, K. and Patziger, M. (2018). On the accuracy of three dimensional flow measurements at low velocity ranges in municipal wastewater treatment reactors. *Flow Measurement and Instrumentation*, 64:39–53.

[Labidi, 2019] Labidi, A. (2019). What is the mach number?

[Lis, 1982] Lis, Z. H. (1982). Two-phase flow measurements with sharp-edged orifices.

[Lockhart and Martinelli, 1949] Lockhart, R. W. and Martinelli, R. C. (1949). Proposed correlation of data for isothermal two-phase, two-component flow in pipes. *Chemical Engineering Progress*, 45(1):39–48.

[Mandhane et al., 1974] Mandhane, J., Gregory, G., and Aziz, K. (1974). A flow pattern map for gas—liquid flow in horizontal pipes. *International Journal of Multiphase Flow*, 1:537–553.

[Melzer et al., 2020] Melzer, S., Munsch, P., Förster, J., Friderich, J., and Skoda, R. (2020). A system for time-fluctuating flow rate measurements in a single-blade pump circuit. *Flow Measurement and Instrumentation*, 71.

[Miller, 2014] Miller, D. (2014). *Internal Flow Systems*. 3rd edition edition.

[Morris, 1985] Morris, S. (1985). Two phase pressure drop across valves and orifice plates. *Proc. European Two Phase Fl ow Group Meeting*.

[NFOGM, 2005] NFOGM (2005). Handbook of multiphase flow metering.

[Orea et al., 2020] Orea, D., Vaghetto, R., Nguyen, T., and Hassan, Y. (2020). Experimental measurements of flow mixing in cold leg of a pressurized water reactor. *Annals of Nuclear Energy*, 140:107137.

[Osman and Ovinis, 2020] Osman, A. B. and Ovinis, M. (2020). A review of in-situ optical flow measurement techniques in the deepwater horizon oil spill.

[Qing et al., 2006] Qing, M., Jinghui, Z., Yushan, L., Haijun, W., and Quan, D. (2006). Experimental studies of orifice-induced wall pressure fluctuations and pipe vibration. *International Journal of Pressure Vessels and Piping - INT J PRESSURE VESSELS PIPING*, 83:505–511.

[Reader-Harris and A, 1996] Reader-Harris and A, S. J. (1996). The orifice plate discharge coefficient equation-the equation for iso 5167-1.

[Simpson et al., 1981] Simpson, H. C., Rooney, D. H., and Grattan, E. (1981). Two phase flow through gate valves and orifice plates.

[Time, 2017] Time, R. W. (2017). *Two phase flow in pipelines*. Department of Petroleum Engineering, Faculty of Science and Technology, University of Stavanger.

[Vemulapalli and Venkata, 2022] Vemulapalli, S. and Venkata, S. K. (2022). Parametric analysis of orifice plates on measurement of flow: A review. *Ain Shams Engineering Journal*, 13:101639.

[Wallis, 1969] Wallis, G. B. (1969). *One-Dimensional Two-Phase Flow*. Mcgraw-Hill, New York.

[White, 2011] White, F. M. (2011). *Fluid Mechanics*. 7th edition.

[Yan and Thorpe, 1990] Yan, Y. and Thorpe, R. (1990). Flow regime transitions due to cavitation in the flow through an orifice. *International Journal of Multiphase Flow*, 16:1023–1045.

[Yan et al., 1988] Yan, Y., Thorpe, R. B., and Pandit, A. B. (1988). Cavitation noise and its suppression by air in orifice flow. page 25 – 39. Cited by: 30.

[Zeghloul et al., 2017] Zeghloul, A., Azzi, A., Saidj, F., Messilem, A., and Azzopardi, B. J. (2017). Pressure drop through orifices for single- and two-phase vertically upward flow - implication for metering. *Journal of Fluids Engineering, Transactions of the ASME*, 139.

[ÇENGEL, 2007] ÇENGEL, J. M. C. Y. A. (2007). *FLUID MECHANICS*.

Appendices

Appendix A

Python Codes

A.1 Interpolation for time step= 0.005 sec

```python
#Import parameters to be used in the project
pressure = pd.read_excel('C:/Users/Sal/orifice 0,5 Beta.xls', '0.76 liquid 10slpm gas')#Example
array = np.array(pressure)
data = traces.TimeSeries()
for i in array:
    data[i[0]] = i[1]
regular_time_series = data.sample(sampling_period=0.005, start=min(array[:, 0]), end=max(array[:, 0]), interpolate='linear') #Interpolation of the values
x = []
y = []
    for i in regular_time_series:
        x.append(i[0])
        y.append(i[1])
```

Listing A.1: Selection of time-frame i.e 0.005s used for this study (only the relevant part of the code is presented)

A.2 Peaks and plots

```python
peaks_x = []
peaks_y = []
for i in range (1, (len (data) - 1)): #using a window
    prev_item = data.get_item_by_index (i - 1) #using a window
```
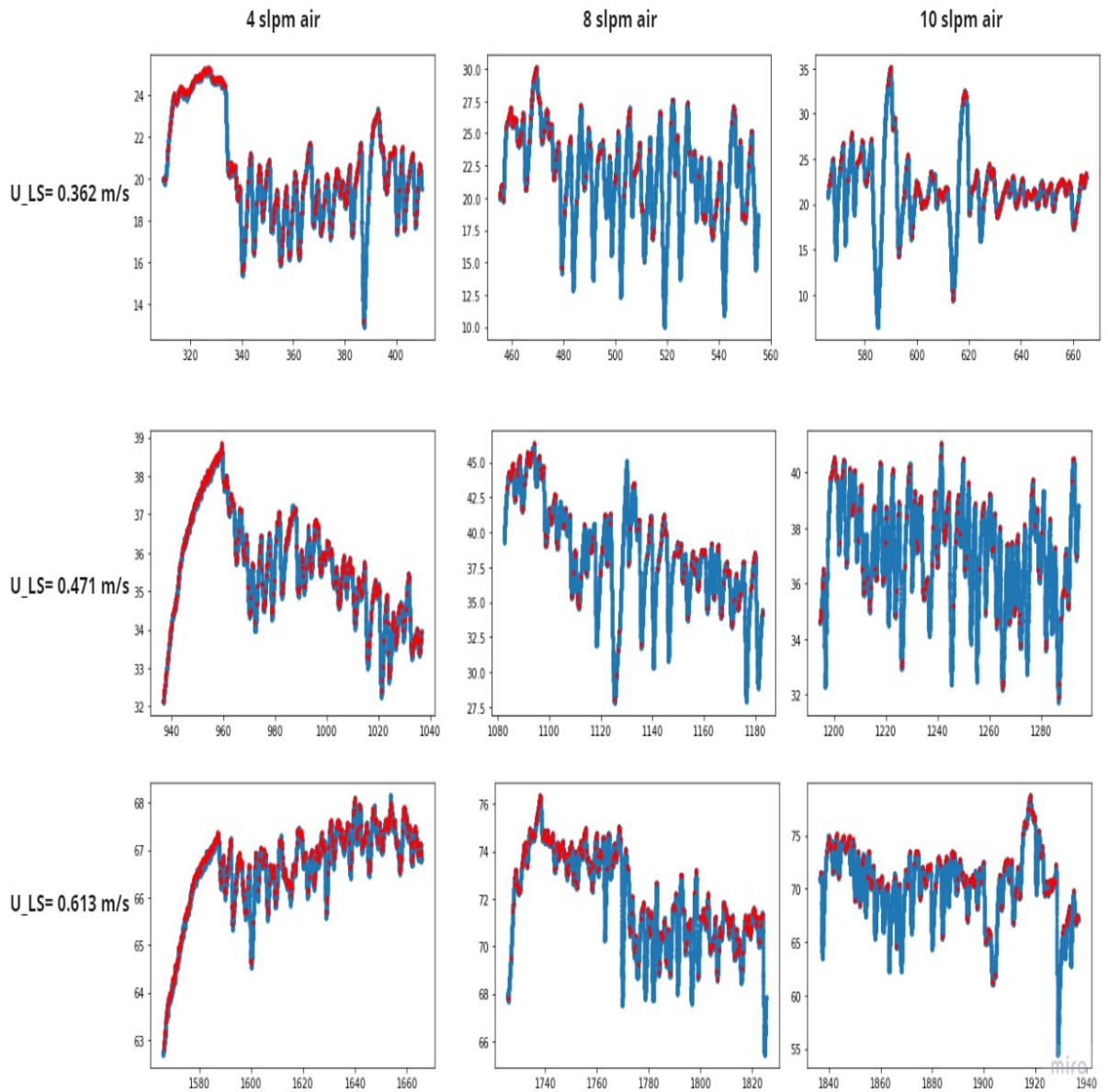
```
6            current_item = data.get_item_by_index(i) #using a window
7            next_item = data.get_item_by_index(i + 1) #using a window
8            if (current_item[1] > prev_item[1] and current_item[1] >
    next_item[1]):
9                peaks_x.append(current_item[0])
10               peaks_y.append(current_item[1])
11           plt.plot(x,y,peaks_x,peaks_y,'ro',marker=".")
12
```

Listing A.2: Peaks to study

A.3   Results from plotting peaks

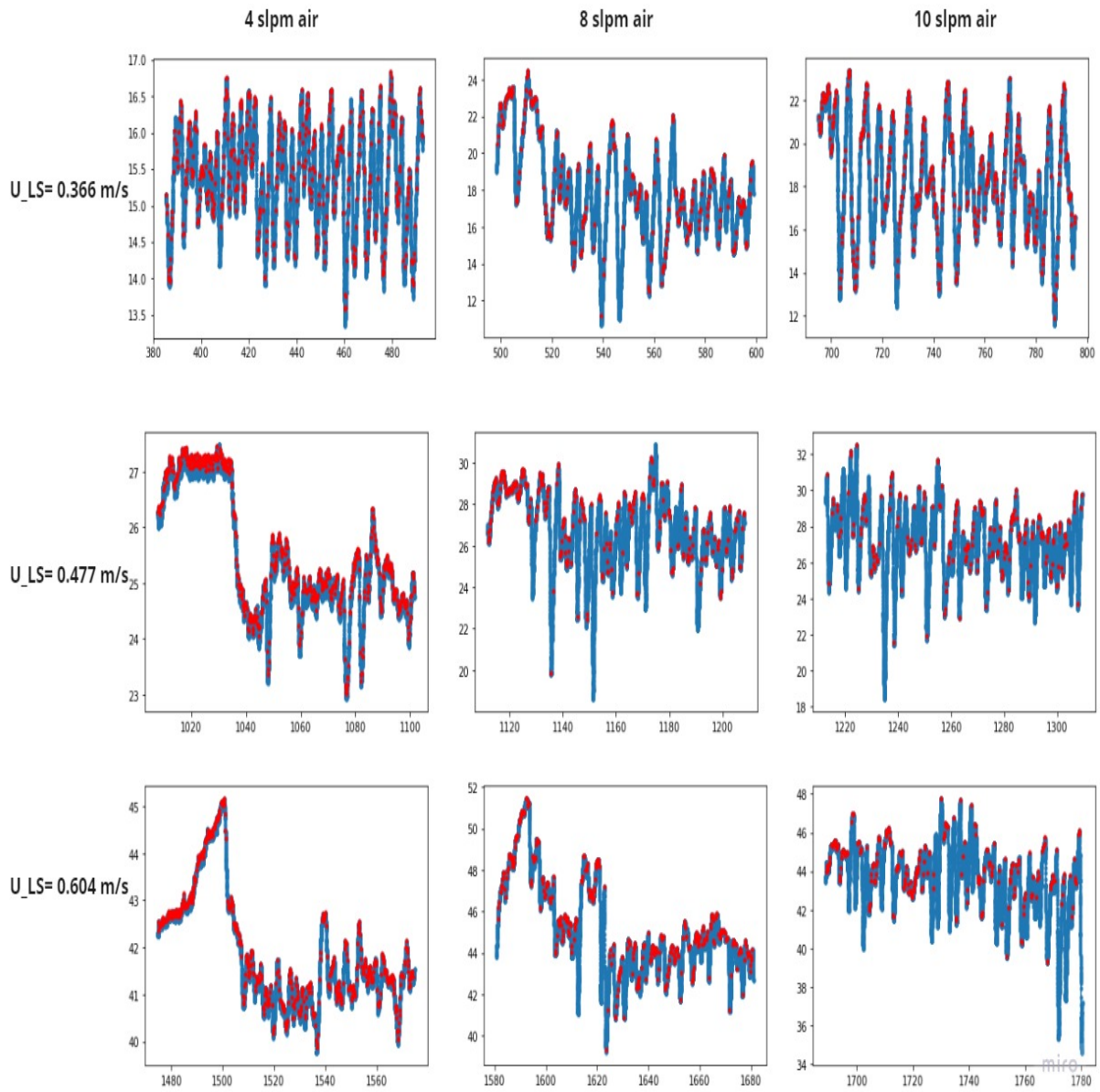**Figure A.1:** Pressure peaks vs. Time for 0.5 β orifice

Figure A.2: Pressure peaks vs. Time for 7-hole orifice

Appendix B

Orifice Meter Equations

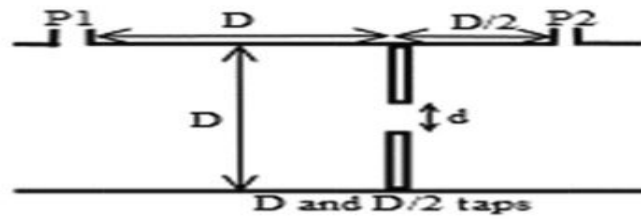## B.1 Orifice equation for two-phase flow

Figure B.1: D and D/2 taps

The following equation is developed from [Fadaei et al., 2021]. From Bernoulli's equation we have:

$$\frac{P_1}{\rho g} + \frac{V_1^2}{2g} + z_1 = \frac{P_2}{\rho g} + \frac{V_2^2}{2g} + z_2 \tag{B.1}$$

where P is pressure, V is velocity, D and d are pipe diameter at zones D and d. Simplifying we get

$$\left[\frac{P_1}{\rho g} + z_1\right] - \left[\frac{P_2}{\rho g} + z_2\right] = \frac{V_2^2 - V_1^2}{2g} \tag{B.2}$$

Where Shrinkage factor is:

$$C_c = \frac{A_2}{A_1} \tag{B.3}$$

where A_2 is the area of orifice plate for d and A_1 is the area of pipe D. The continuity equation

is as follows:

$$A_1 v_1 = A_2 v_2 \tag{B.4}$$

Combining shrinkage factor and continuity equation we get:

$$v_1 = \frac{A_0 C_c}{A_1} v_2 \tag{B.5}$$

Implementing Eq. (B.5) into the Eq. (B.2) we get:

$$v_2 = \frac{\sqrt{2gh}}{\sqrt{1 - \frac{A_2^2}{A_1^2} C_c^2}} \tag{B.6}$$

The flow rate is as follows:

$$Q = A_2 v_2 = A_1 v_2 C_c = \frac{A_1 C_c \sqrt{2gh}}{1 - \frac{A_2^2}{A_1^2} C_c^2} \tag{B.7}$$

Simplifying mass flow:

$$\dot{m} = \rho A_2 \sqrt{\frac{2(P_1 - P_2)}{\rho \left[1 - \frac{A_2^2}{A_1^2}\right]}} \tag{B.8}$$

And the Orifice discharge coefficient is defined as follows:

$$C_D = C_c \frac{\sqrt{1 - \frac{A_2^2}{A_1^2}}}{\sqrt{1 - \frac{A_1^2}{A_1^2} C_c^2}} \tag{B.9}$$

The Orifice equation is as follows:

$$\dot{m} = \frac{C A_2}{\sqrt{1 - \left(\frac{D_2}{D_1}\right)^4}} \sqrt{2\rho(P_1 - P_2)} \tag{B.10}$$

B.2   Excel file for calculations

The following is a screenshot from excel to calculate the flow through orifice.

To modify	Calculated	

Calculations according to ISO 5167

$$q_m = \frac{C}{\sqrt{1-\beta^4}} \, \epsilon \, \frac{\pi}{4} \, d^2 \, \sqrt{2 \, \rho_1 \Delta p}$$

Flow calculation		
Orifice diameter	16	mm
Pipe diameter	40	mm
Ratio	0.4	
Fluid density upstream	997	kg/m3
Expansibility factor	1	1 for liquids For gases calculated with cell L30
Coefficient of discharge	0.65	Cd around 0.65 for orifice plate
Pressure drop	15471	Pa
Flow through orifice	0.735	kg/s

Figure B.2: Excel example to calculate flow rate through orifices